2-1-2016

The Toxicity of the Aggregatibacter Actinomycetemcomitans Cytolethal Distending Toxin Correlates With its Phosphatidylinositol-3,4,5-Triphosphate Phosphatase Activity

Bruce J. Shenker
University of Pennsylvania

Kathleen Boesze-Battaglia
University of Pennsylvania

Monika Damek Scuron
University of Pennsylvania

Lisa P. Walker
University of Pennsylvania

Ali Zekavat
University of Pennsylvania

See next page for additional authors

Recommended Citation

Shenker, B. J., Boesze-Battaglia, K., Scuron, M. D., Walker, L. P., Zekavat, A., & Dlakić, M. (2016). The Toxicity of the Aggregatibacter Actinomycetemcomitans Cytolethal Distending Toxin Correlates With its Phosphatidylinositol-3,4,5-Triphosphate Phosphatase Activity. *Cellular Microbiology, 18* (2), 223-243. http://dx.doi.org/10.1111/cmi.12497

The Toxicity of the Aggregatibacter Actinomycetemcomitans Cytolethal Distending Toxin Correlates With its Phosphatidylinositol-3,4,5-Triphosphate Phosphatase Activity

Abstract

The Aggregatibacter actinomycetemcomitans cytolethal distending toxin (Cdt) induces G2 arrest and apoptosis in lymphocytes and other cell types. We have shown that the active subunit, CdtB, exhibits phosphatidylinositol-3,4,5-triphosphate (PIP3) phosphatase activity, leading us to propose that Cdt toxicity is the result of PIP3 depletion and perturbation of phosphatidylinositol-3-kinase (PI-3K)/PIP3/Akt signalling. To further explore this relationship, we have focused our analysis on identifying residues that comprise the catalytic pocket and are critical to substrate binding rather than catalysis. In this context, we have generated several CdtB mutants and demonstrate that, in each instance, the ability of the toxin to induce cell cycle arrest correlates with retention of phosphatase activity. We have also assessed the effect of Cdt on downstream components of the PI-3K signalling pathway. In addition to depletion of intracellular concentrations of PIP3, toxin-treated lymphocytes exhibit decreases in pAkt and pGSK3β. Further analysis indicates that toxin-treated cells exhibit a concomitant loss in Akt activity and increase in GSK3β kinase activity consistent with observed changes in their phosphorylation status. We demonstrate that cell susceptibility to Cdt is dependent upon dephosphorylation and concomitant activation of GSK3β. Finally, we demonstrate that, in addition to lymphocytes, HeLa cells exposed to a CdtB mutant that retains phosphatase activity and not DNase activity undergo G2 arrest in the absence of H2AX phosphorylation. Our results provide further insight into the mode of action by which Cdt may function as an immunotoxin and induce cell cycle arrest in target cells such as lymphocytes. © 2016 John Wiley & Sons Ltd.

Disciplines

Dentistry

Author(s)

Bruce J. Shenker, Kathleen Boesze-Battaglia, Monika Damek Scuron, Lisa P. Walker, Ali Zekavat, and Mensur Dlakić

Cellular Microbiology (2016) **18**(2), 223–243
doi:10.1111/cmi.12497
First published online 2 September 2015

The toxicity of the *Aggregatibacter actinomycetemcomitans* cytolethal distending toxin correlates with its phosphatidylinositol-3,4,5-triphosphate phosphatase activity

Bruce J. Shenker,[1]* Kathleen Boesze-Battaglia,[2] Monika Damek Scuron,[1] Lisa P Walker,[1] Ali Zekavat[1] and Mensur Dlakić[3]
[1]*Department of Pathology, University of Pennsylvania School of Dental Medicine, Philadelphia, PA, USA.*
[2]*Department of Biochemistry, University of Pennsylvania School of Dental Medicine, Philadelphia, PA, USA.*
[3]*Department of Microbiology and Immunology, Montana State University, Bozeman, MT, USA.*

Summary

The *Aggregatibacter actinomycetemcomitans* cytolethal distending toxin (Cdt) induces G2 arrest and apoptosis in lymphocytes and other cell types. We have shown that the active subunit, CdtB, exhibits phosphatidylinositol-3,4,5-triphosphate (PIP3) phosphatase activity, leading us to propose that Cdt toxicity is the result of PIP3 depletion and perturbation of phosphatidylinositol-3-kinase (PI-3K)/PIP3/Akt signalling. To further explore this relationship, we have focused our analysis on identifying residues that comprise the catalytic pocket and are critical to substrate binding rather than catalysis. In this context, we have generated several CdtB mutants and demonstrate that, in each instance, the ability of the toxin to induce cell cycle arrest correlates with retention of phosphatase activity. We have also assessed the effect of Cdt on downstream components of the PI-3K signalling pathway. In addition to depletion of intracellular concentrations of PIP3, toxin-treated lymphocytes exhibit decreases in pAkt and pGSK3β. Further analysis indicates that toxin-treated cells exhibit a concomitant loss in Akt activity and increase in GSK3β kinase activity consistent with observed changes in their phosphorylation status. We demonstrate that cell susceptibility to Cdt is dependent upon dephosphorylation and concomitant activation of GSK3β. Finally, we demonstrate that, in addition to lymphocytes, HeLa cells exposed to a CdtB mutant that retains phosphatase activity and not DNase activity undergo G2 arrest in the absence of H2AX phosphorylation. Our results provide further insight into the mode of action by which Cdt may function as an immunotoxin and induce cell cycle arrest in target cells such as lymphocytes.

Received 21 April, 2015; revised 22 July, 2015; accepted 26 July, 2015. *For correspondence. E-mail shenker@upenn.edu; Tel. (+1) 215 898 5959; Fax (+1) 215 573 2050.

Introduction

Over the past several years, lipids in general, and phosphatidylinositol-3,4,5-triphosphate (PIP3) in particular, have become recognized for their central role in regulating an array of biological responses; these include cell growth, proliferation and survival, among others (Kraub and Haucke, 2007; Sasaki *et al.*, 2007; Buckler *et al.*, 2008; Huang and Sauer, 2010). PIP3 is normally maintained at low intracellular levels and increases rapidly in response to a variety of signals that involve plasma membrane recruitment and activation of phosphatidylinositol-3-kinase (PI-3K). Normal cell function requires that PIP3 levels be tightly regulated; three degradative enzymes, PTEN, SHIP1 and SHIP2, have been shown to play critical roles in this capacity (Krystal, 2000; March and Ravichandran, 2002; Seminario and Wange, 2003). The tumour suppressor phosphatase, PTEN (*p*tase and *t*ensin homolog deleted on chromosome *ten*), hydrolyses PIP3 to phosphatidylinositol-4,5-biphosphate (PI-4,5-P2). SHIP1 (*s*rc *h*omology 2-containing inositol ihosphatase) and SHIP2 are inositol 5-phosphatases (IP5P); whereas SHIP2 is ubiquitously expressed, SHIP1 appears to be found in a limited subset of cells including most immune cells. Both SHIP enzymes hydrolyse PIP3 to phosphatidylinositol-3,4-biphosphate (PI-3,4P2) and inositol 1,3,4,5-tetrakisphosphate to inositol 1,3,4-triphosphate. Collectively, these enzymes contribute to regulation of the PI-3K/PIP3/Akt signalling pathway.

Over the course of our investigations, we have demonstrated that *Aggregatibacter actinomycetemcomitans*, a

putative pathogen implicated in the aetiology and pathogenesis of localized juvenile periodontitis, produces an immunotoxin that affects human T cells (Shenker *et al*., 1982b; 1990; 1999). This toxin was shown to interfere with normal cell cycle progression, resulting in G2 arrest as well as inducing apoptosis (Shenker *et al*., 1995). Moreover, we have shown that the active toxin is the product of the cytolethal distending toxin (Cdt) operon (Shenker *et al*., 1999). Cdts are a family of heat-labile protein cytotoxins produced by several different bacterial species including *Campylobacter jejuni*, Shigella species, *Haemophilus ducreyi*, *A. actinomycetemcomitans* and diarrhoeal disease-causing enteropathogens such as some *Escherichia coli* isolates (Scott and Kaper, 1994; Okuda *et al*., 1995; Pickett *et al*., 1996; Comayras *et al*., 1997; Mayer *et al*., 1999; Shenker *et al*., 1999). The Cdt operon contains three genes, *cdtA*, *cdtB* and *cdtC*, which specify three polypeptides with molecular masses of 18, 32 and 20 kDa respectively. Cdt holotoxin functions as an AB2 toxin, where subunits CdtA and CdtC comprise the binding (B) unit and CdtB the active subunit. Moreover, CdtC binds to the plasma membrane of cells via cholesterol in the context of lipid rafts (Boesze-Battaglia *et al*., 2009). It should also be pointed out that Carette *et al*. (2009) demonstrated that cell mutants lacking sphingomyelin synthase are resistant to CdtB. These results suggest that CdtB may be involved in lipid metabolism as lipid rafts and sphingomyelin-controlled protein scaffolds are important for lipid signalling in cells: either lipid rafts are important for CdtB entry into cells, or lipid raft integrity is necessary for CdtB function once inside of the cell. Thus, it is particularly noteworthy that we recently demonstrated that CdtB is capable of hydrolysing PIP3 and appears to function as an IP5P similar to the SHIP enzymes (Shenker *et al*., 2007). Hence, as lipid rafts often serve as signalling platforms, we predict that CdtB is endocytosed into the cell, allowing it to access the cytoplasmic face of the cell membrane and to PIP3 pools.

Our studies have led us to propose that CdtB-induced cell cycle arrest and apoptosis is the result of PIP3 depletion and perturbation of the PI-3K/PIP3/Akt signalling cascade. The relationship between CdtB and SHIP is not surprising because the initial observations of Dlakic (2001) indicate sequence and structural homology between CdtB and a larger group of divergent enzymes that include IP5P. These enzymes have been predicted, based on structural analysis, to be similar in fold and mechanism to DNase I and related metal-dependent phosphohydrolases (Drayer *et al*., 1996; Mitchell *et al*., 1996; Woscholski and Parker, 1997; Majerus *et al*., 1999; Tsujishita *et al*., 2001). To further explore this relationship and the role of PIP3 phosphatase activity in Cdt-mediated toxicity, we have extended our investigation to an analysis of the amino acid residues that comprise the catalytic pocket and that contribute to substrate binding. Furthermore, we now demonstrate that Cdt-treated lymphocytes exhibit alterations in the PI-3K signalling cascade consistent with the action of the toxin acting as an IP5P. Finally, we demonstrate a relationship between activation of GSK3β, PIP3 content and susceptibility to Cdt-induced G2 arrest.

Results

Analysis of CdtB substrate binding mutants

Based on sequence and structural comparisons, it has been proposed that the active Cdt subunit, CdtB, shares catalytic residues and a similar reaction mechanism with a large group of functionally diverse Mg^{2+}-dependent phosphoesterases (Dlakic, 2000). DNase I was the first structurally characterized member of this enzyme superfamily (Lahm and Suck, 1991); subsequent structural characterization of IP5P and CdtB confirmed the initial prediction (Tsujishita *et al*., 2001; Nesic *et al*., 2004; Yamada *et al*., 2006). An alignment of these three structures shows striking conservation of catalytic and divalent ion-chelating residues, despite low overall sequence identity (Fig. 1A). As a general rule, all enzymes in this superfamily use the same catalytic residues to hydrolyse phosphate esters, and their specific function is determined by additional, non-catalytic residues that line up the active site and recognize the correct substrate(s). Thus, these additional residues allow for substrate specificity even though other substrates sometimes can be accommodated, albeit with lower affinity, and are usually converted with considerably lower activity. CdtB appears to be an enzyme with strong PIP3 phosphatase activity and weak DNase activity (Shenker *et al*., 2007), which implies that PIP3 is its primary substrate; in this scenario, DNA would be an incidental substrate that can be acted upon only with much lower activity.

Our previous studies focused on mutating catalytic residues (Shenker *et al*., 2007); however, this approach did not give a clear answer as to whether CdtB is primarily a phosphatase or a nuclease because both activities are likely to be abolished. Instead, mutations targeting substrate binding and other non-catalytic functions of the protein are likely to provide clear distinction between the two possible activities. Therefore, we generated several CdtB mutants that involve amino acid substitutions in residues that correspond to the putative active site and likely to be involved in substrate binding (Table 1); these residues are R117, R144 and A163. Docking analysis using IP3 as a substrate raised the possibility that R117 interacts with C3 phosphate of IP3 and that R144 forms a hydrogen bond with either the C4 or C5 phosphate; we predicted that mutations of either of these two arginines to alanine would reduce phosphatase activity while possibly not compromising DNase activity (Figs. S1 and S2). A163

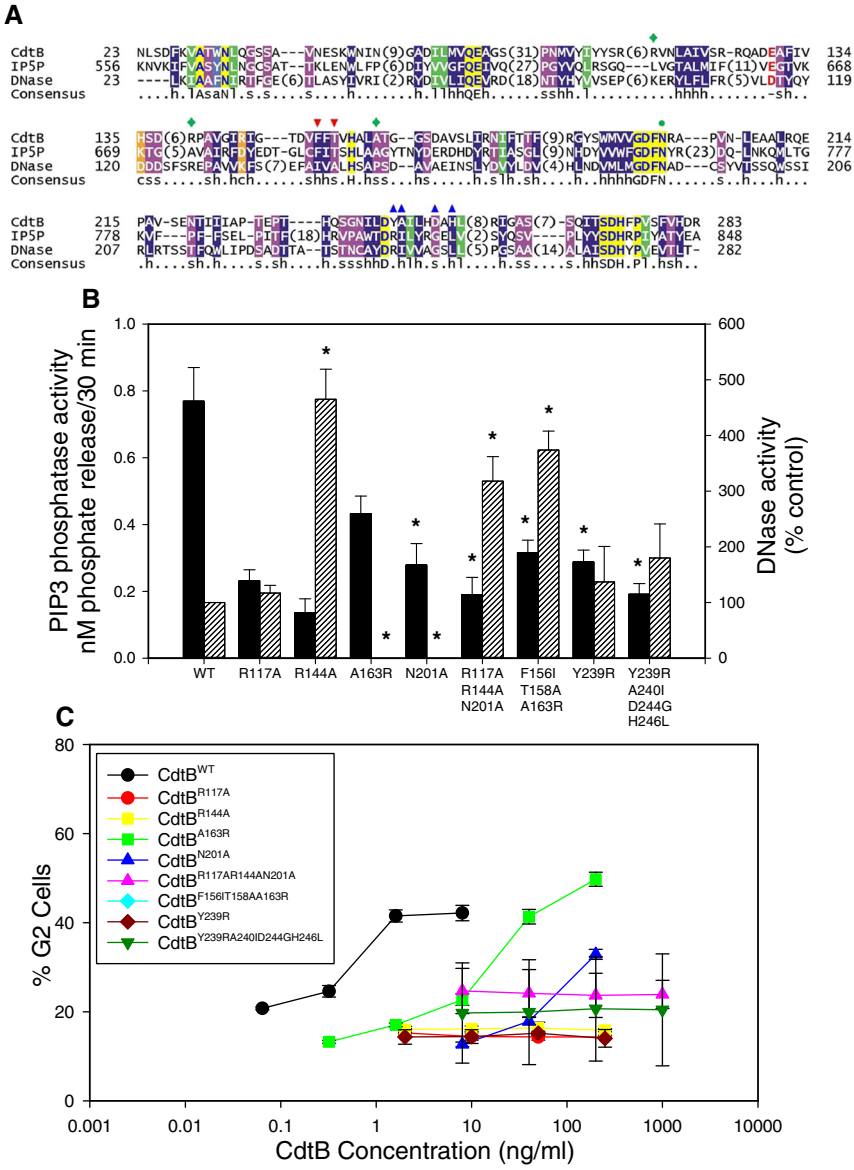

Fig. 1. Analysis of CdtB mutants for PIP3 phosphatase, DNase and toxic activities. Panel A shows the structural alignment of CdtB (PDB code 2f2f_B, accession number Q7DK12), inositol polyphosphate 5-phosphatase (IP5P) (PDB code 1i9y_A, accession number O43001) and DNase I (PDB code 2dnj_A, accession P00639), which was obtained by MUSTANG and modified by hand after visual inspection of structures. Numbering in the alignment refers to full-length proteins. The consensus line indicates the conservation of small (s), aliphatic (l), hydrophobic (h), charged (c), positive (+) and negative (−) residues, while identical residues are shown as capital letters. Numbers in parentheses within the alignment indicate how many residues were omitted either because of long insertions not shared by all proteins or because structures could not be reliably aligned in those regions. Amino acids mutated in this study were divided into three groups: residues predicted to be involved in substrate binding (marked by green diamonds above the alignment), residues near the catalytic H160 that are conserved in CdtB and IP5P but not DNase I (red triangles pointing down) and residues near the catalytic D238 that are conserved in IP5P and DNase I but not CdtB (blue triangles pointing up). The catalytic N201 is marked by a green dot because in some experiments it was combined with binding mutants. Each mutant was analysed for PIP3 phosphatase activity (panel B), DNase activity (panel B) and the ability to induce G2 arrest in Jurkat cells (panel C). PIP3 phosphatase activity was assessed in the presence of 0.25 μM and is expressed as nanomolar phosphate release from PIP3 per 30 min. DNase activity was assessed as described in *Materials and methods*; numbers represent the % control ($CdtB^{WT}$) as mean ± SEM of each mutant to convert supercoiled plasmid DNA to the relaxed form. The ability of the mutants to induce G2 arrest is described in *Experimental procedures section* (Shenker *et al.*, 2005). The percentage of G2 cells is plotted versus CdtB concentration; cells exposed to medium exhibited 14% G2 cells. Results are the mean ± SEM of three experiments. The asterisk indicates statistical significance ($p < 0.05$) when compared with $CdtB^{WT}$.

was chosen because it interacted differently with IP3 and IP2 based on docking experiments, and we wanted to assess its role in substrate binding specificity. The R117 and R144 mutants were already tested for DNase (Nesic *et al.*, 2004), but not phosphatase activity; we decided to include them for comparison. Likewise, we included another residue, N201, which is associated with the catalytic site and is conserved in all three proteins (Fig. 1A);

Table 1. CdtB mutant constructs.

Plasmid	Primer	Sequence[a]
pGEMCdtB^{R117A}	P1	GATGTTGGGGCAAAC**GC**AGTGAACTTAGCTATCG
	P2	CGATAGCTAAGTTCACT**GC**GTTTGCCCCAACATC
pGEMCdtB^{R144A}	P3	CTGTGCTTCAATCT**GC**CCCGGCAGTAGGTATCC
	P4	GGATACCTACTGCCGGG**GC**AGATTGAAGCACAG
pGEMCdtB^{A163R}	P5	CAGTGCATGCTTTG**AA**CACAGGTGGTTCTGATGCGG
	P6	CCGCATCAGAACCACCTGTG**TT**CAAAGCATGCACTG
pGEMCdtB^{N201A}	P7	GGATGGTTGTTGGTGATTTC**GC**TCGTGCGCCGG
	P8	CCGGCGCACGA**GC**GAAATCACCAACAACCATCC
pGEMCdtB$^{R117A•R144A•N201A}$	P9	CTGTGCTTCAATCT**GC**CCCGGCAGTAGGTATCC
	P10	GGATACCTACTGCCGGG**GC**AGATTGAAGCACAG
pGEMCdtB$^{F156I•T158A•A163R}$	P11	CGCATTGGTACTGATGTA**A**TTTTT**G**CAGTGCATGCTTTG
	P12	CAAAGCATGCACTG**C**AAAAA**T**TACATCAGTACCAATGCG
pGEMCdtB^{Y239R}	P13	CGGTCCGGTAATATTTTAGAT**CG**TGCGATTTTACATGACGCAC
	P14	GTGCGTCATGTAAAATCGCA**CG**ATCTAAAATATTACCGGACCG
pGEMCdtB$^{Y239R•A240I•D244G•H246L}$	P15	CGGTCCGGTAATATTTTAGAT**CGTATC**ATTTTACATGACGCAC
	P16	GTGCGTCATGTAAAAT**GATA**CG**A**TCTAAAATATTACCGGACCG
	P17	ATCATTTTACATG**G**CGCAC**T**TTTACCACGTCGA
	P18	TCGACGTGGTAAA**A**GTGCG**C**CATGTAAAATGAT

[a] Bold letters in the sequence indicate nucleotide substitutions.

docking analysis demonstrated close proximity of this residue to inositol within the substrate.

We constructed plasmids that express the following CdtB mutants: CdtB^{R117A}, CdtB^{R144A}, CdtB^{A163R}, CdtB^{N201A} and the triple mutant CdtB$^{R117A•R144A•N201A}$. Mutants were first assessed for PIP3 phosphatase activity (Fig. 1B). Although the CdtB^{R117A}, CdtB^{R144A} and CdtB$^{R117A•R144A•N201A}$ mutants exhibited detectable levels of phosphatase activity, the values were significantly below that observed with CdtB^{WT} (0.77 ± 0.10 nM of phosphate release per 30 min); CdtB^{N201A} exhibited phosphatase activity that was higher than the other three mutants (0.28 ± 0.06 nM of phosphate release per 30 min) but also statistically lower than that observed for the wild-type protein. In contrast, CdtB^{A163R} exhibited phosphatase activity that was reduced relative to CdtB^{WT} (0.43 ± 0.05 nM of phosphate release per 30 min); however, this difference was not statistically different from that observed for the CdtB^{WT}. Additionally, the mutants were analysed for DNase activity (Fig. 1B). Relative to CdtB^{WT} (100%), DNase activity exhibited by CdtB^{R117A} was increased slightly (117 ± 14% of wild type) while CdtB^{R144A} and CdtB$^{R117A•R144A•N201A}$ exhibited increased activity to 465 ± 54% and 318 ± 44 %, respectively, of the activity observed with CdtB^{WT}. In contrast, CdtB^{N201A} and CdtB^{A163R} did not exhibit detectable DNase activity. It is noteworthy that CdtB^{A163R} is the first non-catalytic mutant that retains most of the PIP3 phosphatase activity while being unable to cleave DNA. Finally, CdtB mutants were assessed for their ability to induce cell cycle arrest (Fig. 1C). It should be noted that, as previously reported, the ability of CdtB to induce G2 arrest requires the presence of CdtA and CdtC (Shenker *et al.*, 2004; 2005). Thus, these experiments were performed in the presence of CdtA and CdtC under conditions that we have previously demonstrated to result in an active toxin complex. CdtB^{A163R} retained toxic activity as exposure to 6 and 40 ng ml^{-1} of the mutant resulted in 23 ± 1.3% and 41.3 ± 1.6% G2 cells; this compares with the effect of CdtB^{WT} at 0.32 (24.6 ± 1.3% G2 cells) and 1.6 ng ml^{-1} (41.5 ± 1.7% G2 cells). Untreated control cells exhibited 14% G2 cells. In contrast, CdtB^{N201A} induced 17.9 ± 0.8 and 32.9 ± 1.1% G2 cells at 40 and 200 ng ml^{-1} of mutant protein respectively. It should be noted that the other two CdtB mutants failed to exhibit the ability to induce cell cycle arrest in Jurkat cells at concentrations tested (up to 1 μg ml^{-1}).

Analysis of CdtB mutants close to the active sites of CdtB, IP5P and DNase

Alignment of CdtB, IP5P and DNase I demonstrates a number of residues that are conserved in two out of the three proteins (Fig. 1A). We first focused on regions close to catalytic residues that are conserved in both CdtB and IP5P; these residues were mutated to the residues found in DNase I. A plasmid was constructed that expressed a protein with three residues modified, CdtB$^{F156I•T158A•A163R}$; PIP3 phosphatase activity of this mutant was significantly reduced to 0.31 ± 0.03 nM of phosphate release per 30 min compared with 0.77 ± 0.1 nM of phosphate release for CdtB^{WT} (Fig. 1B). In contrast, this mutant exhibited increased DNase activity to 374 ± 34% of control values (Fig. 1B). CdtB$^{F156I•T158A•A163R}$ was unable to induce G2 arrest at any concentrations tested (Fig. 1C). It should be noted that an additional construct expressing CdtB$^{F156I•T158A}$ exhibited similar properties as the triple mutant. Next, two additional plasmids were constructed to express CdtB mutants that target residues conserved in

both DNase I and IP5P; we mutated these residues to match DNase I residues at those positions. These mutants include $CdtB^{Y239R}$ and $CdtB^{Y239R•A240I•D244G•H246L}$; both mutants demonstrated significantly reduced PIP3 phosphatase activity: 0.19 ± 0.03 ($CdtB^{Y239R}$) and 0.32 ± 0.03 ($CdtB^{Y239R•A240I•D244G•H246L}$) (Fig. 1B). Figure 1B also shows the results of DNase analysis for these mutants; $CdtB^{Y239R}$ exhibited nuclease activity comparable with $CdtB^{WT}$ (137 ± 64%) while $CdtB^{Y239R•A240I•D244G•H246L}$ exhibited an increase in nuclease activity (180 ± 61%). Analysis of the ability of the mutants to induce G2 arrest in Jurkat cells (Fig. 1C) indicates that $CdtB^{Y239R}$ and $CdtB^{Y239R•A240I•D244G•H246L}$ were unable to induce cell cycle arrest at any concentration tested. Therefore, mutants that disrupt phosphatase activity of CdtB also disrupt its cytotoxic properties, even when the nuclease activity of those same mutants is improved or unaffected.

Effect of Cdt on downstream PI-3K signalling

In order to further define the role for lipid phosphatase activity in Cdt-mediated toxicity, we first demonstrate that the toxin is indeed capable of altering intracellular levels of substrate and product, PIP3 and PI-3,4P2, respectively, in both the Jurkat cell line and in primary lymphocytes activated with mitogen. As shown in Fig. 2A, Jurkat cells treated with Cdt exhibited a dose-dependent decrease in PIP3. Baseline levels of PIP3 in untreated cells were 3.7 ± 1.0 pmol per 10^6 cells. In contrast, cells treated with 50 pg ml^{-1} of Cdt for 1 h exhibited a reduction to 2.7 ± 0.5 pmol per 10^6 cells; PIP3 levels further declined to 1.4 ± 0.3 and 0.8 ± 0.4 pmol per 10^6 cells in the presence of 500 and 5000 pg ml^{-1} of Cdt. The decrease in PIP3 was also time dependent (Fig. 2B); a 21% reduction was observed within 30 min in cells exposed to 50 pg ml^{-1} of Cdt (2.6 ± 0.5 pmol per 10^6 cells) versus that observed in control cells (3.3 ± 0.3 pmol per 10^6 cells). PIP3 levels continued to decline over time (30–120 min) with levels reduced by 42% (60 min) and 61% (120 min). Toxin-treated Jurkat cells were also assessed for changes in the enzymatic product of Cdt-mediated PIP3 de-phosphorylation, PI-3,4P2. Cdt (50 pg ml^{-1}) caused a time-dependent increase in the intracellular levels of PI-3,4P2 (Fig. 2B). Cells exhibited a 28% increase in the phosphatidylinositol-diphosphate within 30 min of exposure to toxin (0.84 ± 0.06 pmol per 10^6 cells) over that observed in control cells (0.65 ± 0.06 pmol per 10^6 cells). Intracellular levels of PI-3,4P2 continued to increase over time (30–120 min), reaching a more than threefold increase at 120 min (2.1 ± 0.1 pmol per 10^6 cells). The increase in PI-3,4P2 was specific as intracellular concentrations of PI-4,5-P2 were not altered (Fig. 2B).

Mitogenic stimulation of human peripheral blood mononuclear cells (HPBMC) is known to lead to activation of the PI-3K signalling cascade and a rapid rise in PIP3 levels (Liscovitch and Cantley, 1992; Coers *et al*., 1995; Cantley and Neel, 1999; Buckler *et al*., 2008; Huang and Sauer, 2010). We have previously shown that Cdt is capable of inhibiting mitogen-induced proliferation of HPBMC (Shenker *et al*., 2000). Therefore, we determined if Cdt was able to prevent this mitogen-induced increase in PIP3. HPBMC were pre-treated with Cdt (or medium) for 60 min and then stimulated with phytohaemagglutinin (PHA) (Fig. 2C). Cells were then assessed for PIP3 levels at varying time intervals (0–120 min). Control HPBMC incubated for 60 min with PHA exhibited a 44% increase in PIP3 (Fig. 2C); these concentrations remained elevated for at least 2 h. In contrast, HPBMC pre-treated with Cdt failed to exhibit an increase in PIP3, and instead, PIP3 levels were reduced 40% and 60% at 60 and 120 min respectively. Similar results were observed with cells activated with anti-CD3 and anti-CD28 monoclonal antibodies (data not shown).

The PI-3K signalling pathway controls cellular functions via the activation of protein kinases and the downstream phosphorylation of multiple substrates. In the next series of experiments, we focused on the effect of Cdt on the downstream targets of PIP3: Akt and GSK3β. Jurkat cells were treated with 200 pg ml^{-1} of Cdt for 0–4 h, and the levels of Akt, pAkt, GSK3β and pGSK3β analysed by Western blot. As shown in Fig. 2D and E, Akt phosphorylation (S473) was reduced to 63 ± 12.3% of control values at 1 h and significantly reduced to 48.7 ± 9.3% and 45.5 ± 11.6% of control values at 2 and 4 h respectively. Akt levels were not significantly altered at any time point. Additionally, pGSK3β (S9) was reduced to 65.3 ± 15.1% of control levels at 1 h and significantly reduced to 55.7 ± 6.0% and 47.6 ± 6.1% of control values at 2 and 4 h respectively. No significant changes in GSK3β levels were observed during the 4 h of exposure to Cdt. Similarly, Cdt was able to block the mitogen (PHA)-induced increase in pGSK3β that occurs upon HPBMC activation. As shown in Fig. S3, PHA increased pGSK3β to 146% of that observed in untreated control cells; exposure to 50, 250 and 1000 pg ml^{-1} Cdt reduced pGSK3β to 123%, 80% and 34% of that observed in control cells respectively. In order to obtain information on changes in pAkt and pGSK3β in individual cells, we extended our studies to include analysis by immunofluorescence and flow cytometry. As shown in Fig. 3, Jurkat cells treated with Cdt exhibit a dose-dependent reduction in the percentage of cells containing detectable pAkt (S473); values ranged from 82% in control cells down to 21% in cells exposed to 10 ng ml^{-1} of Cdt. Flow cytometric analysis of pGSK3β also indicates a dose-dependent reduction in the percentage of cells containing the phosphorylated kinase; values ranged from 78% positive cells in the control population to 55% (0.1 ng ml^{-1} of Cdt), 34% (1.0 ng ml^{-1} of Cdt) and 12% (10.0 ng ml^{-1} of Cdt).

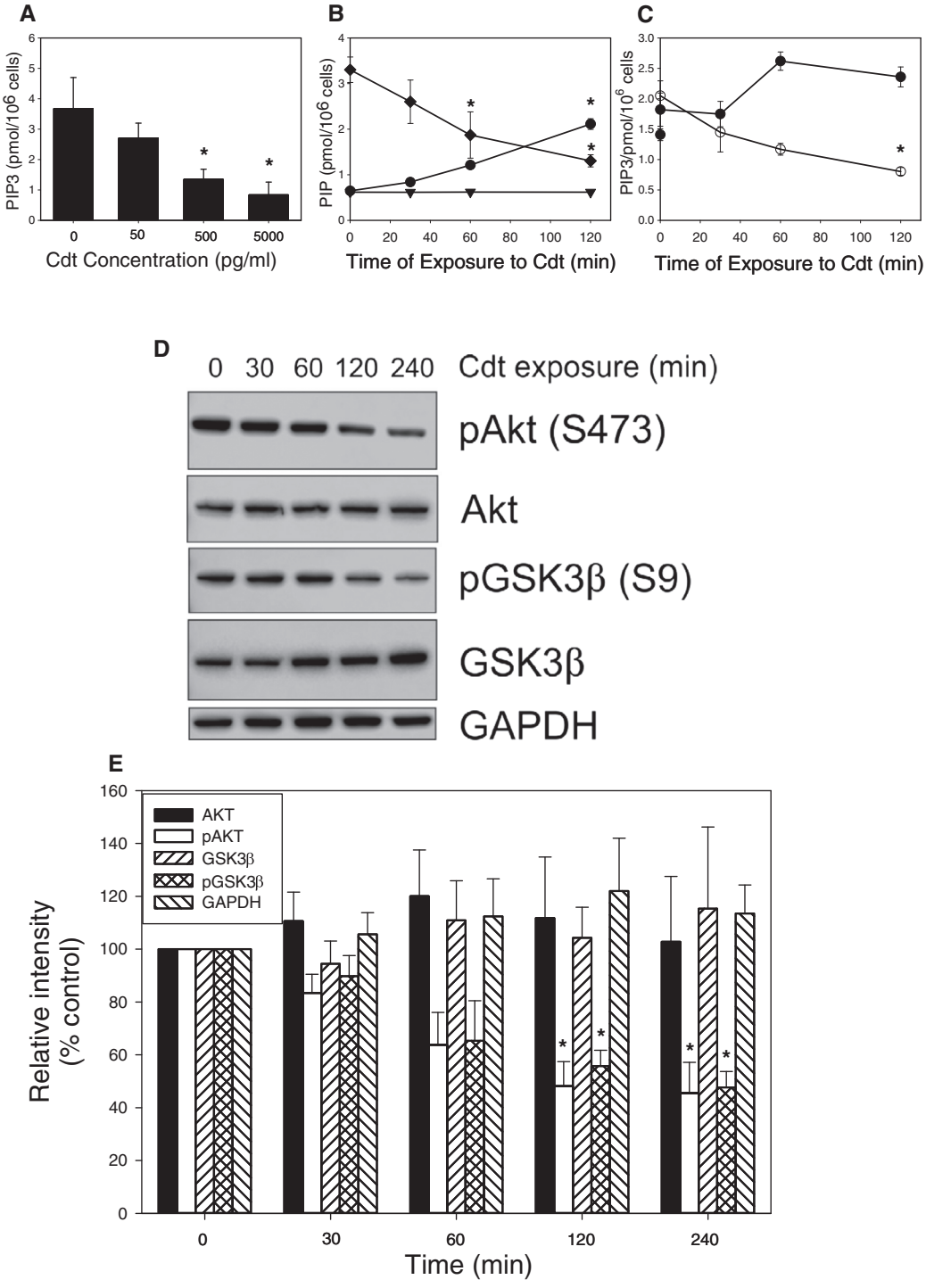

Fig. 2. Effect of Cdt on PI-3K signalling in Jurkat cells and HPBMC. Jurkat cells were exposed to Cdt holotoxin as indicated, harvested, PIs extracted and measured by enzyme-linked immunosorbent assay. Panel A shows the effect of varying amounts of Cdt on Jurkat cells after 1 h of exposure. Jurkat cells were also exposed to Cdt (50 pg ml^{-1}) for varying time periods (panel B); levels of PIP3 (diamonds), PI-3,4P2 (circles) and PI-4,5-P2 (triangles) are plotted. Panel C shows the results for HPBMC pre-incubated in medium (solid circles) or with Cdt (open circles; 50 pg ml^{-1}) for 1 h. HPBMC were then activated for varying periods of time in the presence of PHA. Results are plotted as picomole PIP3 or PIP2 per 10^6 cells; data represent the mean ± SEM for three experiments. The asterisk indicates statistical significance ($p < 0.05$) when compared with untreated control (panels A and B) and to PHA control (panel C), Panel D shows a representative Western blot of the effect of Cdt on Akt and GSK3β phosphorylation. Jurkat cells were treated with Cdt (200 pg ml^{-1}) for 2 h and then analysed by Western blot for pAkt (S473), Akt, pGSK3β (S9), GSK3β and GAPDH as a loading control. Panel E: Blots from three experiments were analysed by scanning densitometry and are expressed as a percentage of the relative intensity of untreated control cells; mean ± SEM for three experiments are plotted. The asterisk indicates statistical significance ($p < 0.05$) when compared with untreated control cells.

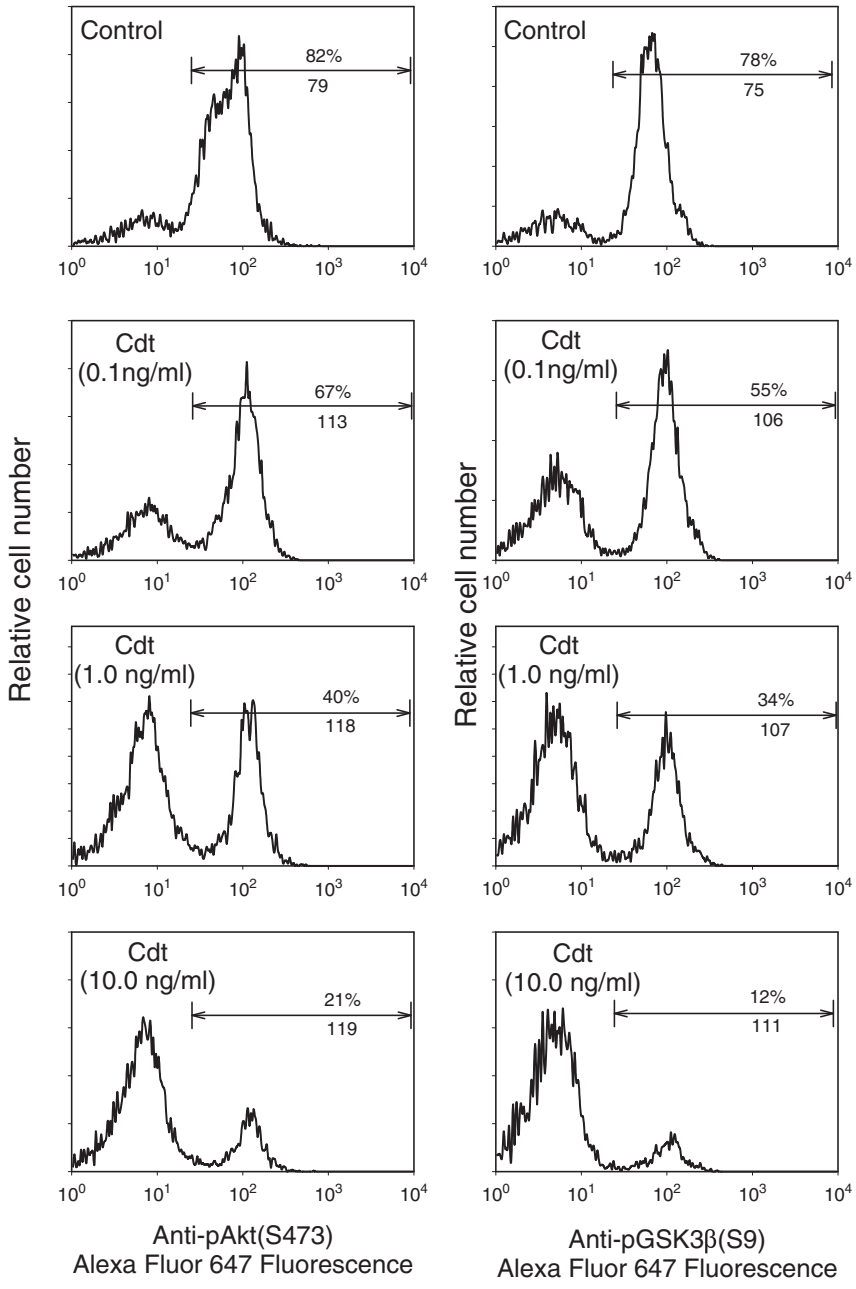

Fig. 3. Flow cytometric analysis of pAkt and pGSK3β in Cdt-treated cells. The effect of Cdt on pAkt (S473) (left panels) and pGSK3β (S9) (right panels) in individual cells is shown. Cells were treated with Cdt holotoxin (0–10 ng ml^{-1}) and analysed by flow cytometry following immunofluorescence staining. Bars indicate the analysis gate for positively stained cells; the percentage of positive cells as well as their mean channel fluorescence is indicated. Results are representative of three experiments.

In addition to Western blot and flow cytometric analysis of the phosphorylation status of Akt and GSK3β, we also assessed Cdt-treated Jurkat cells (4 h) for both Akt and GSK3β kinase activity. The active form of Akt (pAkt) was isolated from cell extracts by immunoprecipitation and activity assessed by monitoring phosphorylation of GSK. As shown in Fig. 4A, Akt obtained from Cdt-treated cells exhibited reductions in kinase activity relative to control cells: 65 ± 11% (0.1 ng ml^{-1} of Cdt), 63 ± 18% (1.0 ng ml^{-1} of Cdt) and 45 ± 13% (10 ng ml^{-1} of Cdt). Likewise, GSK3β was isolated by immunoprecipitation and then monitored for kinase activity by utilizing labelled ATP to measure ^{32}P incorporation into a synthetic substrate. Cells exposed to toxin exhibited a dose-dependent increase in GSK3β kinase activity (Fig. 4B); activity increased from 57% (0.1 ng ml^{-1} of Cdt) to 206% above control levels

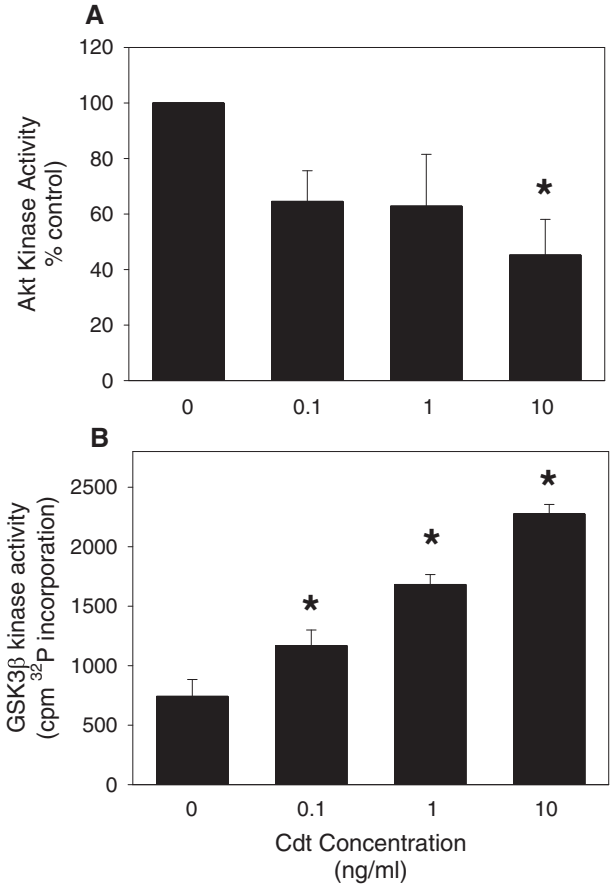

Fig. 4. Effect of Cdt on Akt and GSK3β kinase activity. Jurkat cells were treated with 0.1, 1.0 and 10 ng ml^{-1} of Cdt holotoxin for 4 h. Panel A shows Akt kinase activity following pAkt immunoprecipitation from solubilized cells. Akt kinase activity was measured by monitoring GSK3β phosphorylation *in vitro*; results are expressed as a percentage of control, and the mean ± SEM are plotted. GSK3β kinase activity was measured in similarly treated cells followed by immunoprecipitation of the kinase; GSK3β activity was determined by monitoring the utilization of ^{32}P-ATP to phosphorylate a synthetic substrate. Data are plotted as ^{32}P (cpm) incorporation versus Cdt concentration; results represent the mean ± SEM for three experiments. The asterisk indicates statistical significance ($p < 0.05$) when compared with untreated control cells.

(10 ng ml^{-1} of Cdt). In order to determine if the Cdt-induced increase in GSK3β activity was required for the toxin to induce cell cycle arrest, we employed four cell permeable inhibitors of the kinase. As shown in Fig. 5, Jurkat cells treated with Cdt alone (50 pg ml^{-1}) exhibited an increase in the percentage of G2 cells to 58% while untreated cells contained 19% G2 cells. Each of the GSK3β inhibitors reduced the percentage of G2 cells in the presence of Cdt: 29% (LiCl), 25% (GSK inhibitor X), 25% (GSK inhibitor XII) and 15% (GSK inhibitor XV). In addition to Jurkat cells, the GSK inhibitor X prevented Cdt-induced G2 arrest in PHA-activated HPBMC (Fig. S4).

Several investigators have proposed that Cdt-mediated toxicity in non-lymphoid cells is the direct result of DNA damage resulting from DNase activity associated with CdtB, leading to activation of the DNA damage response (DDR) (Cortes-Bratti *et al*., 2001a; Frisan *et al*., 2002; Li *et al*., 2002; Hassane *et al*., 2005). To address these disparate findings and determine if the DDR plays a role in Cdt-induced cell cycle arrest in lymphocytes, we employed two Ataxia telangiectasia mutated (ATM) inhibitors: KU60019 and KU55933. Because we previously demonstrated that H2AX phosphorylation was not directly due to the action of Cdt in Jurkat cells (Shenker *et al*., 2006), we chose to utilize a different lymphoid cell line for these experiments, CCRF-CEM, an acute lymphoblastic leukaemia cell line. CCRF-CEM cells were exposed to 200 pg ml^{-1} of Cdt, a dose optimized for G2 arrest. As shown in Fig. 6I, this dose of Cdt resulted in 42.0 ± 1.1% G2 cells after 16 h; this compares with 16.0 ± 2.6% in control (untreated) cells. Neither of the inhibitors had an effect on Cdt-induced G2 arrest; the percentage of G2 cells was 39.1 ± 2.3% and 40.9 ± 0.1% in cells pre-treated with 10 μM of KU60019 or 10 μM of KU55933, respectively, and then exposed to toxin. These results are consistent with our failure to detect an effect of Cdt on pH2AX as the mean channel fluorescence (MCF) of CCRF-CEM cells stained with anti-pH2AX antibody conjugated to fluorescein isothiocyanate and analysed by flow cytometry was unchanged in the presence of toxin relative to control values (Fig. 6A–D). To verify the validity of our approach and the effectiveness of the ATM inhibitors, CCRF-CEM cells were similarly treated with etoposide. In contrast to Cdt, treatment with 0.5 μM of etoposide induced pH2AX staining as these cells exhibited an MCF of 213 vs 38 in control cells. As shown in Fig. 6E–H, the ATM inhibitors reduced pH2AX to an MCF of 147 (KU60019) and 150 (KU55933). Moreover, etoposide alone resulted in G2 arrest (45 ± 3.9%); cell cycle arrest was reduced to 29.8 ± 6.8 and 28.1 ± 2.6% G2 cells in the presence of KU60019 and KU55933 respectively (Fig. 6I).

The failure of Cdt to induce phosphorylation of H2AX in CCRF-CEM cells and the inability of ATM kinase inhibitors to block toxin-induced cell cycle arrest are consistent with a Cdt mode of action involving PI-3K signalling blockade and inconsistent with a mechanism involving activation of the DDR. To determine if non-lymphoid cells were affected in a similar fashion, we assessed and compared CdtB^{WT} with CdtB^{A163R}, the mutant that retained phosphatase and toxic activities and that lost DNase activity, and CdtB^{R144A}, the mutant that lost phosphatase and toxic activities but exhibited an increase in DNase activity, for their ability to both induce G2 arrest and H2AX phosphorylation in a commonly used experimental Cdt target, HeLa cells. As shown in Fig. 7A–D and I, treatment of HeLa cells for 24 h with 25 ng ml^{-1} of either CdtB^{WT} or CdtB^{A163R} (in the presence of CdtA and CdtC subunits as described) resulted in 77.1 ± 11.0% and 75.6 ± 11.7% G2 cells. In contrast, control cells and HeLa cells treated with CdtB^{R144A}

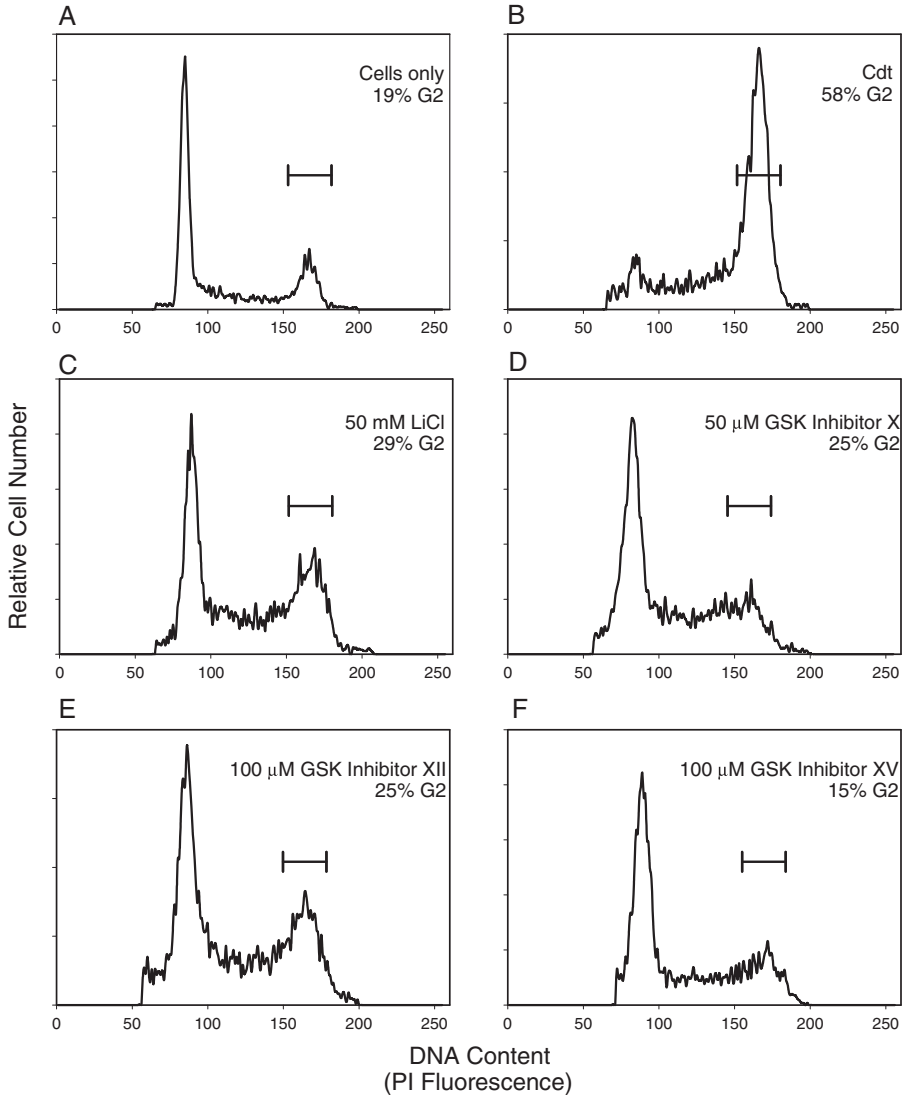

Fig. 5. Effect of GSK3β inhibitors on Cdt-induced cell cycle arrest. Jurkat cells were pre-treated with medium, LiCl, GSK inhibitor X, XI or XV for 1 h followed by the addition of Cdt holotoxin (50 pg ml^{-1}). Sixteen hours later, the cells were harvested, stained with propidium iodide and analysed for cell cycle distribution by flow cytometry. Representative results of three experiments are shown: cells only (A), Cdt alone (B), LiCl and Cdt (C), GSK inhibitor X and Cdt (D), GSK inhibitor XI and Cdt (E) and GSK inhibitor XV and Cdt (F). Inhibitors alone had no effect on cell cycle. Area under bars represent the G2 population; numbers represent the percentage of G2 cells.

exhibited 12.9±3.1% and 17.5±1.3% G2 cells. H2AX phosphorylation was assessed 16 h after exposure to toxin as this was the earliest time that we observed pH2AX in HeLa cells. In a representative experiment, the wild-type CdtB subunit induced an increase in the MCF of cells stained with anti-pH2AX-fluorescein isothiocyanate to 81 vs 15 in untreated cells (Fig. 7E–H). Cumulative results from multiple experiments demonstrated a statistically significant increase in pH2AX fluorescence of 375% over that observed in control cells (set at 100%). In contrast, CdtB^{A163R} had a marginal effect on pH2AX fluorescence, raising the MCF in a representative experiment to 22. Based upon multiple experiments, treatment of HeLa cells with CdtB^{A163R} resulted in a 37.3 ± 2.0% increase in pH2AX fluorescence over that observed in control cells; this difference was not statistically significant. However, the reduction in pH2AX fluorescence observed with CdtB^{A163R} versus CdtB^{WT} was statistically significant (Fig. 7I). Likewise, CdtB^{R144A} failed to induce pH2AX in HeLa cells; these cells exhibited an MCF of 18 (Fig. 7H), and the aggregate data indicate pH2AX fluorescence equivalent to control cells (105 ± 8%). In summary, we show that the CdtB^{A163R} mutant, in which phosphatase and DNase activities are decoupled, can induce G2 arrest without causing DNA damage and further that the CdtB^{R144A} mutant, which exhibits reduced phosphatase and a significant increase in DNase activity, is not able to induce either G2 arrest or H2AX phosphorylation.

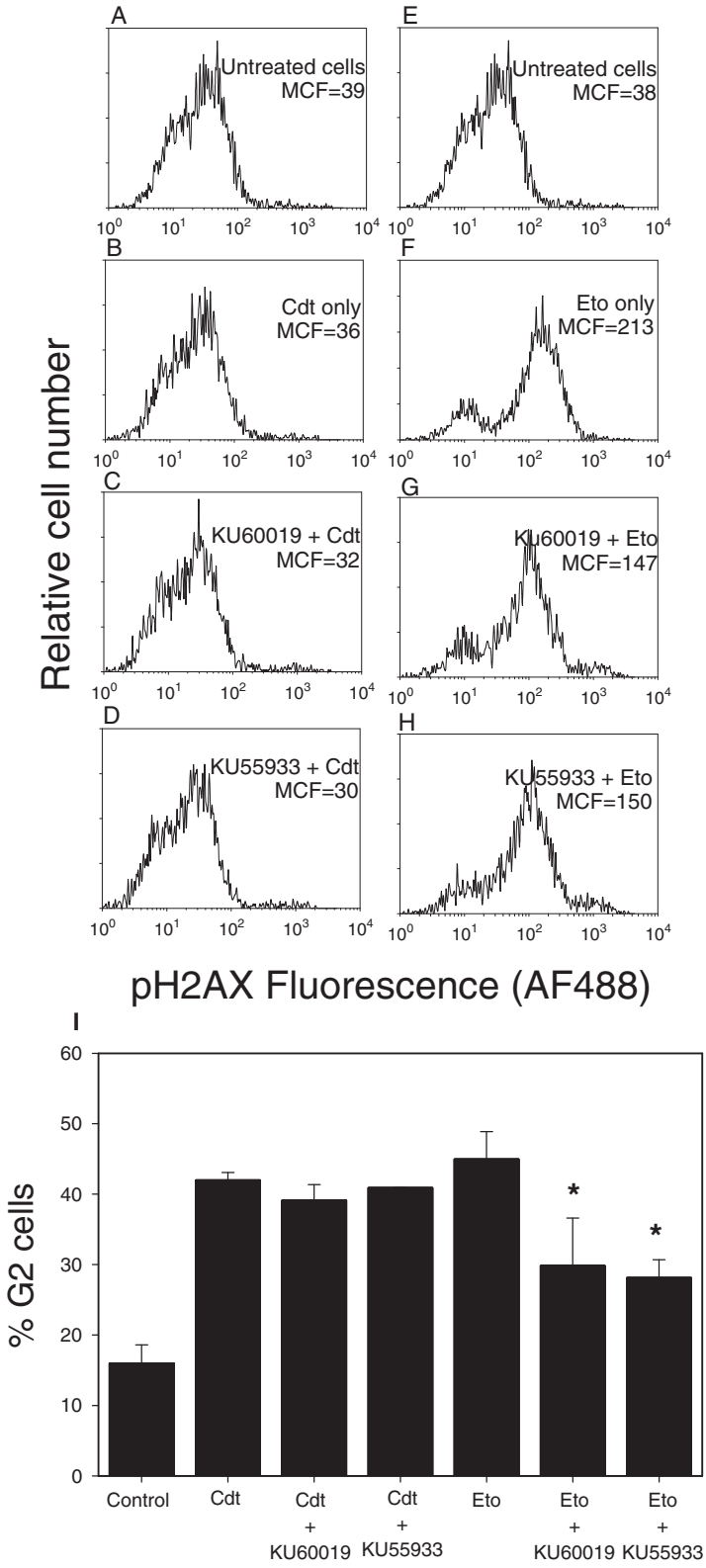

Fig. 6. Effect of ATM kinase inhibitors on Cdt-induced toxicity. CCRF-CEM cells were treated with medium (control), Cdt holotoxin (200 pg ml^{-1}) or etoposide (0.5 μM) for 4 h to measure pH2AX fluorescence (panels A–H) or G2 arrest (panel I). In some instances, cells were pre-treated with 10 μM of ATM kinase inhibitors: KU60019 or KU655933. Representative (of three experiments) pH2AX fluorescence is shown (panels A–H), and the mean ± SEM for the percentage of G2 cells for three experiments is shown panel I; the asterisk indicates statistical significance ($p < 0.05$) when compared with cells treated with etoposide.

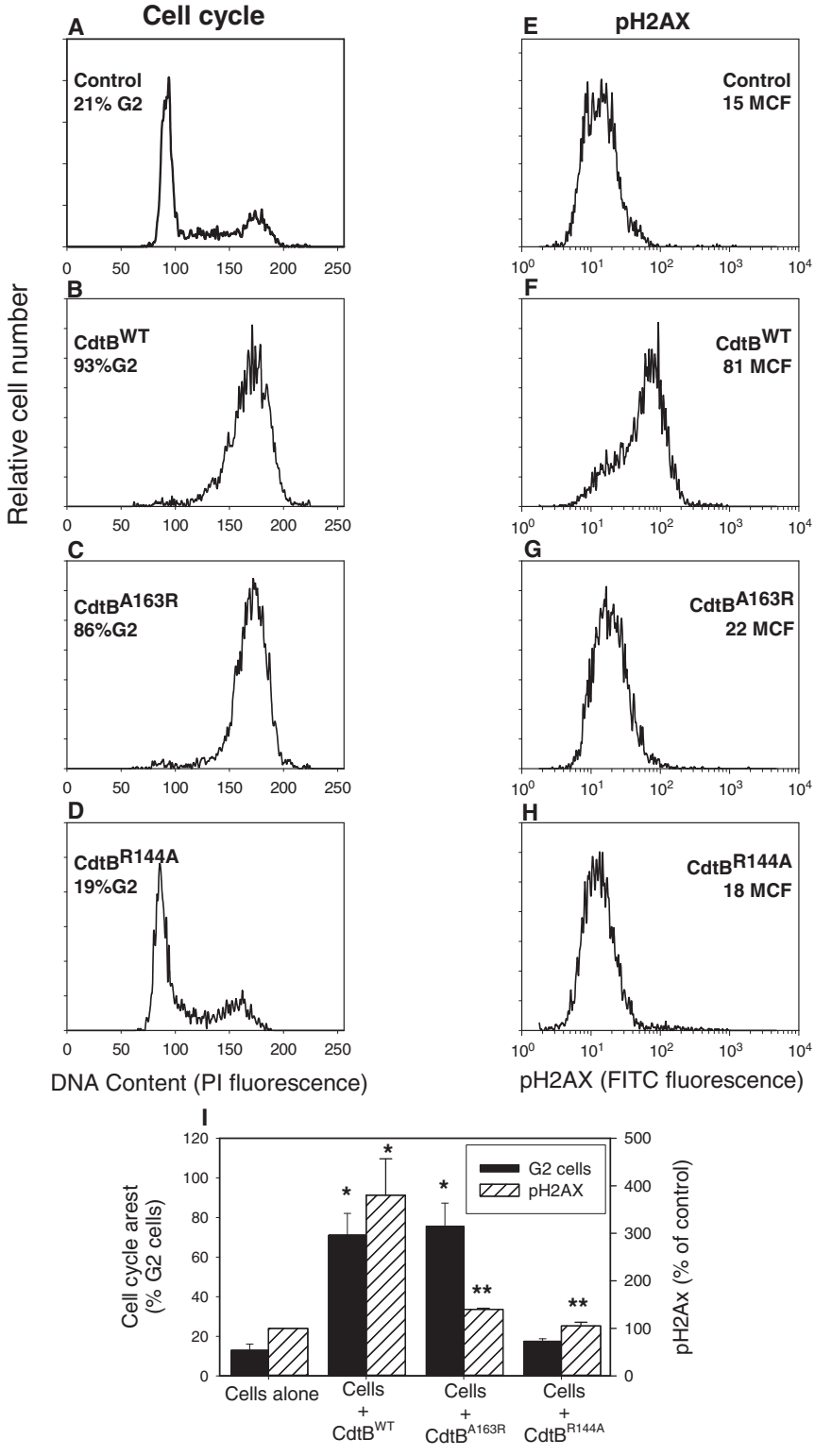

Fig. 7. Comparison of the effect of CdtB^{WT}, CdtB^{A163R} and CdtB^{R144A} on cell cycle and pH2AX in HeLa cells. HeLa cells were treated with medium alone (panels A and E), CdtA and CdtC in the presence of CdtB^{WT} (panels B and F), CdtB^{A163R} (panels C and G) or CdtB^{R144A} (panels D and H). Representative results for cells analysed for G2 arrest at 24 h (panels A–D) or pH2AX at 16 h (panels E–H) are shown. The mean ± SEM for three experiments is shown in panel I; solid bars represent results of cell cycle analysis (%G2 cells), and hatched bars represent the mean channel fluorescence intensity for pH2AX of three experiments expressed as a percentage of control; the single asterisk indicates statistical significance ($p < 0.05$) when compared with untreated control cells, and the double asterisk indicates statistical significance ($p > 90.05$) when compared with cells treated with CdtB^{WT} alone.

In the last series of experiments, we explored the possibility that Cdt alters PI-3K signalling in HeLa cells in a manner similar to that observed with lymphoid cells. The effect of the toxin was first assessed on PIP3 levels. As shown in Fig. 8A, baseline levels of PIP3 in HeLa cells was 4.5 ± 0.4 pmol per 10^6 cells; these values decreased to 3.6 ± 0.6 and 3.2 ± 0.3 pmol per 10^6 cells at 4 h after exposure to 5 and 50 ng ml^{-1} of Cdt. Increasing the toxin concentration to 500 ng ml^{-1} did not cause a further decline in PIP3 levels. Similar results were observed for pGSK3β; in the presence of CdtB^{A163R} and CdtB^{R144A}, phosphorylation of this kinase was reduced to 67% of control values (Fig. S5). The ability of GSK inhibitor XV was then tested for its ability to block cell cycle arrest induced by both CdtB^{WT} and CdtB^{A163R} (Fig. 8B). HeLa cells were treated with 25 ng ml^{-1} of CdtB peptide in the presence of Cdt subunits A and C as described; cell cycle distribution was assessed 24 h later. Exposure to CdtB^{WT} and CdtB^{A163R} resulted in 77.7 ± 7.3 and 82.8 ± 4.4% G2 cells respectively. The addition of GSK inhibitor XV prior to the addition of toxin blocked cell cycle arrest; the percentage of G2 cells in the presence of inhibitor was 18.2 ± 2.4 (CdtB^{WT}) and 20.5 ± 1.4% G2 (CdtB^{A163R}).

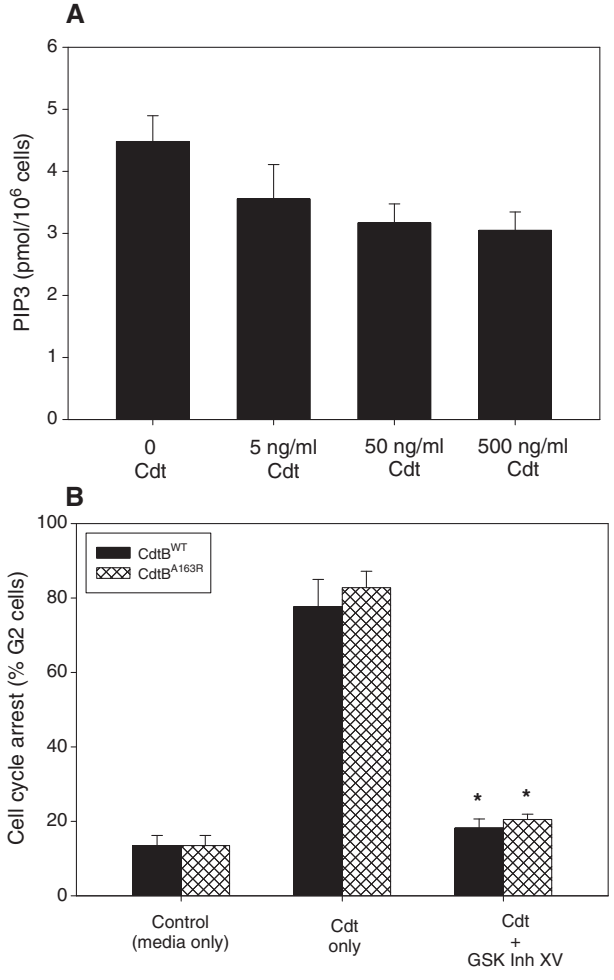

Fig. 8. Effect of Cdt on PIP3 levels in HeLa cells and the ability of GSK3β inhibitor to block toxicity. Panel A: HeLa cells were exposed to Cdt holotoxin as indicated, harvested, PIs extracted and measured by enzyme-linked immunosorbent assay. Bars represent mean ± SEM of three experiments; the asterisk indicates statistical significance ($p < 0.05$) when compared with untreated control cells. Panel B: HeLa cells were exposed to medium alone, 25 ng ml^{-1} CdtB^{WT} or CdtB^{A163R} (in the presence of 25 ng ml^{-1} of each CdtA and CdtC) alone or toxin in the presence the GSK inhibitor XV. Cell were analysed for cell cycle distribution 24 h later. The mean ± SEM for the percent of G2 cells is plotted; the asterisk indicates statistical significance ($p < 0.05$) when compared respectively with cells treated with either CdtB^{WT} or CdtB^{A163R}.

Discussion

There is general agreement that exposure of susceptible target cells to Cdt holotoxin leads to irreversible G2 arrest and eventually apoptosis (Gelfanova *et al*., 1999; Cortes-Bratti *et al*., 2001b; Shenker *et al*., 2001; Ohara *et al*., 2004). However, the nature of the early events leading to toxicity is not clear and are likely dependent upon the underlying molecular mechanism(s) by which the active Cdt subunit, CdtB, interacts with subcellular targets. In this regard, the Cdt holotoxin was recently crystallized and analysed by X-ray crystallography (Nesic *et al*., 2004; Yamada *et al*., 2006). Analysis reveals that CdtB exhibits structural similarity with a group of functionally unrelated metalloenzymes, which includes IP5P and DNase I, among others. Despite the lack of significant pairwise sequence identity, structural similarity was predicted on the basis of sensitive multiple sequence alignments as an extension of an earlier discovery of homology between the nucleases and bacterial sphingomyelinase (Tsujishita *et al*., 2001). Analysis of CdtB indicates that its structure can be superimposed on IP5P with a root mean-square deviation (RMSD) of 3.5 Å over 183 Cα atoms; this compares with a structural overlap of CdtB with DNase I with an RMSD of 3.1 Å over 207 Cα atoms (Shenker *et al*., 2007). The bias in the literature towards rationalizing CdtB function was initially partially based on structural homology with DNase I and has obscured the fact that its protein fold, and most likely the reaction mechanism, is also shared with many proteins within the superfamily of metalloenzymes (Dlakic, 2000; 2001). Indeed, both DNase I and IP5P are phosphoesterases, and it is likely that the specific function of each of these enzymes is dependent upon the substrate(s) that can be accommodated within the active site. Thus, it was not surprising that we were able to demonstrate that CdtB exhibits robust PIP3 phosphatase activity (Shenker *et al*., 2007).

To further explore the role of PIP3 phosphatase activity in Cdt-mediated toxicity, we extended our studies to include CdtB mutants of residues that we predict to be associated with the active site and likely to be involved in substrate binding: R117, R144 and A163 (summarized in

Table 2). Docking analysis using IP3 as a substrate suggested that R144 forms a hydrogen bond with either the C4 or C5 phosphate, which led us to predict that mutation of the arginine to alanine would reduce phosphatase activity while not altering DNase activity. Indeed, the CdtB^{R144A} mutant exhibited reduced PIP3 phosphatase activity and cytotoxicity while DNase activity increased more than fourfold. Moreover, mutation of this site to bulky residues such as tyrosine or lysine (R144Y and R144K) rather than the small alanine resulted in the loss of DNase activity; this is consistent with a reduction of space available to accommodate DNA binding (data not shown). We previously reported that CdtB^{R117A} exhibits loss of DNase activity as well as toxicity (Shenker *et al*., 2011), and now we demonstrate decreased phosphatase activity for this mutant. Our docking analysis suggests that R117 interacts with C3 phosphate of IP3 consistent with our failure to detect any product with the CdtB^{R117A} mutant (Shenker *et al*., 2007). The A163 residue was predicted to be involved in substrate binding, and we expected that mutation of this residue would result in a change in inositol phosphate specificity. We did not observe a change in specificity and observed a modest, but not statistically significant, reduction in phosphatase activity and concomitant decline in toxicity; in contrast, DNase activity was significantly reduced to levels that were not detectable. N201 is a residue found among the catalytic residues and is conserved in all of the metalloenzymes in this family (Dlakic, 2000); this amino acid was mutagenized along with our predicted substrate-binding residues primarily to provide comparison with previous studies (Nesic *et al*., 2004). Our studies indicate that in addition to the loss of both phosphatase and DNase enzymatic activity, the CdtB^{N201A} mutant also lost the ability to induce cell cycle arrest as we observed a minor increase in G2 cells at the highest concentration tested for this mutant (200 ng ml^{-1}) (Tsujishita *et al*., 2001). Lastly, a combination of R117, R144 and N201 mutants was the same as reported by Nesic *et al*. (2004); these authors showed that the triple binding mutant, CdtB$^{R117A•R144A•N201A}$, lost toxicity but retained DNase activity. Our observations are similar as this triple mutant lost toxicity and further lost PIP3 phosphatase activity. It should be noted that in our hands this mutant not only retained DNase activity as reported by Nesic *et al*. (2004) but also exhibited a threefold increase over that observed with CdtB^{WT}. Therefore, our results confirm in a qualitative sense previous observations by Nesic *et al*. (2004) and extend them by linking the loss of CdtB mutant toxicity to the loss of phosphatase activity, which we believe is the primary activity of CdtB.

Table 2. Summary of CdtB mutant activity.

CdtB mutant	DNase activity[a]	PIPase activity[a]	Toxicity[a]
CdtB^{R117A}	Unchanged	↓	↓
CdtB^{R144A}	↑	↓	↓
CdtB^{A163R}	↓	Unchanged	Unchanged
CdtB^{N201A}	↓	↓	↓
CdtB$^{R117A•R144A•N201A}$	↑	↓	↓
CdtB$^{F156I•T158A•A163R}$	↑	↓	↓
CdtB^{Y239R}	Unchanged	↓	↓
CdtB$^{Y239R•A240I•D244G•H246L}$	↑	↓	↓

[a] Activity is relative to CdtB^{WT}.

Additional residues were targeted for mutation based on the following two criteria: (1) proximity to CdtB catalytic residues (in particular H160 and D238) as we tried to increase the likelihood that they are part of the substrate-binding active site and (2) residues that are either conserved in both CdtB and IP5P but not in DNase I or residues that are conserved in IP5P and DNase I but not in CdtB (in both cases, CdtB residues were mutated into corresponding DNase I residues). Our rationale was that if PIP3 phosphatase was the main function of CdtB, making CdtB mutants that resemble DNase I would improve its DNase I activity while impairing its PIP3 phosphatase and cytotoxicity. There are several residues close to catalytic H160 that are conserved in CdtB and IP5P but not DNase I. The double mutant, CdtB$^{F156I•T158A}$, converted residues to those found in DNase I; as predicted, this mutant exhibited almost a doubling of DNase activity as well as decreases in both toxicity and PIP3 phosphatase activity. Introducing a third mutation, CdtB$^{F156I•T158A•A163R}$, yields a mutant protein with greater DNase activity, reduced phosphatase and toxic activities. The last group of mutations involved changing residues close to catalytic D238 that were common to both IP5P and DNase I (Y239, D244, H246 and A240); these were again mutated into corresponding residues of DNase I. The first of these, CdtB^{Y239R}, is positioned some distance away from the presumed binding site according to our docking analysis. We predicted that this mutation should not affect the catalytic pocket; this was true for DNase activity; however, both phosphatase and toxic activities were reduced, suggesting that this residue must be important for CdtB function. Two additional double mutants were generated involving replacement of residues in CdtB to those conserved in both DNase and IP5P. Again, our expectation was that phosphatase activity and toxicity would be reduced and DNase activity elevated. However, CdtB$^{Y239R•A240I}$ and CdtB$^{D244G•H246L}$ exhibited a loss in all three activities (data not shown). Interestingly, all four mutations were combined into a single protein, CdtB^{Y239RA240ID244GH246L}, which resulted in a loss in both PIP3 phosphatase activity and toxicity while DNase activity was increased over that observed with CdtB^{WT}.

Mutation analyses clearly demonstrate that Cdt immunotoxicity and PIP3 phosphatase activity correlated qualitatively for all mutants tested, whereas DNase activity

correlates with toxicity only for the catalytic N201 mutant (summarized in Table 2). As the crystal structure of CdtB is known, we have based our study on specific residues that we predicted would affect substrate binding rather than protein structure. For example, R117, R144 and A163 residues are part of the binding site based upon docking analysis (supporting information). Thus, we are reasonably confident that these mutants are not disrupting the hydrophobic core of CdtB, as all these residues are close to the surface and are unlikely to be important for protein packing and its structural integrity. For the remaining residues that were mutated, we cannot completely exclude the possibility that some mutants may affect protein stability. Yet our speculation is that these mutations are not structurally compromising the protein for two reasons: (1) the mutations were performed to substitute for residues that are already present in related proteins such as DNase I; and (2) whatever the effect of these mutations, it is unlikely to be catastrophic in structural terms because most of them improve DNase I activity and diminish only the phosphatase activity of the resulting mutant protein, which was our rationale for introducing them in the first place.

Taken as a whole, our mutagenesis studies yield two clear conclusions: (1) all mutants diminish PIP3 phosphatase activity of CdtB to some degree, which is to be expected if this is its main enzymatic function; and (2) the majority of mutants improve DNase activity without improving its cytotoxicity, indicating that DNase function of CdtB is secondary. Given the differences between DNA and lipid phosphates in terms of sizes and overall structures, it stands to reason that they will never be equally good enzymatic substrates for any single enzyme. At the same time, both molecules have phosphate esters among their functional groups and likely can be hydrolysed to at least some extent by many enzymes that belong to the same superfamily as CdtB and DNase I (Dlakic, 2000). Unlike mutation of catalytic residues, which typically abolish both PIP3 phosphatase and DNase activity (Shenker *et al*., 2007), we identified mutations in non-catalytic residues that reduce the potency of CdtB as a phosphatase while increasing its DNase activity. It should be noted, however, that a single mutation cannot completely switch enzyme specificity between two different substrates. Therefore, the R144A mutant with $>$400% nuclease activity of the wild-type CdtB and only ~25% of the wild-type CdtB PIP3 phosphatase activity is, in relative terms, still much better as phosphatase than nuclease. We speculate that similar mutations can be made in DNase I that would reduce its nuclease activity while improving its ability to hydrolyse other phosphate esters.

Consistent with the mutation results are our observations that the PI-3K/PIP3/Akt signalling pathway is perturbed by CdtB. Evidence of perturbation of this signalling pathway is supported by our observation that within the first 2 h of exposure to toxin, Jurkat cells exhibit a decline in substrate, PIP3, levels and a concomitant increase in enzymatic product, PI-3,4-P2. Likewise, the toxin was able to block mitogen-induced elevations of PIP3 in HPBMC. Immediately downstream of PIP3 is the critical kinase, Akt, which is normally phosphorylated and activated as a result of PI-3K stimulation and elevations in PIP3. Cdt-mediated depletion of PIP3 was accompanied by a decrease in pAkt, which was both time and dose dependent (the latter not shown); these changes were demonstrated by both Western blot and flow cytometry and confirmed by demonstrating a concomitant decrease in kinase activity.

In addition to changes in Akt phosphorylation, we also observed a reduction in the phosphorylation of the downstream target of pAkt, GSK3β. In contrast to Akt, de-phosphorylation of GSK3β results in a concomitant increase in its kinase activity. GSK3β is a serine/threonine kinase that was initially discovered as an inhibitor of glycogen synthase but has also been implicated in the regulation of inflammation, cell proliferation and apoptosis, among others (Luo, 2009; Rayasam *et al*., 2009). Thus, our observation that GSK3β inhibitors were able to reduce both Jurkat cell and HPBMC susceptibility to Cdt-induced G2 arrest is consistent with the known effects of PI-3K signalling blockade in general, and GSK3β in particular, in regulating cell growth (Buckler *et al*., 2008; Yuan and Cantley, 2008; Huang and Sauer, 2010).

It should be noted that several investigators have suggested that CdtB functions as a DNase, thereby causing DNA degradation leading to activation of the DDR, G2 checkpoint and cell cycle arrest (Lara-Tejero and Galan, 2000; Cortes-Bratti *et al*., 2001b; Frisk *et al*., 2001; Frisan *et al*., 2003) (Cortes-Bratti *et al*., 2001a; Li *et al*., 2002; Guerra *et al*., 2008). These effects were observed in a number of cell lines exposed to relatively high concentrations of Cdt, up to 20 $\mu g\,ml^{-1}$, and include HeLa cells, HEp-2 cells, CHO cells and keratinocytes, among others. Additional evidence for DNase activity in CdtB mode of action is based upon this subunit's ability to denature or relax supercoiled plasmid DNA *in vitro* (Elwell and Dreyfus, 2000; Elwell *et al*., 2001; Mao and DiRienzo, 2002; Frisan *et al*., 2003; Nesic *et al*., 2004). Interestingly, we and others have demonstrated that CdtB exhibits very low DNase activity relative to bovine DNase I ($<$0.01%; Elwell and Dreyfus, 2000; Shenker *et al*., 2001; Nesic *et al*., 2004), perhaps explaining the requirement for high doses of toxin to induce DNA strand breaks. Additionally, several of the earlier studies did not discriminate between direct DNase activity associated with Cdt and the possibility of indirect effects whereby toxin treatment leads to activation of endogenous DNase. Indeed, our own studies on lymphocytes support the notion that the DNA fragmentation we and others have reported in

association with exposure of Cdt results from activation of the apoptotic cascade (Gelfanova *et al*., 1999; Shenker *et al*., 2001; Nalbant *et al*., 2003; Thelastam and Frisan, 2004). Nonetheless, we investigated the possibility that the DDR was also activated in lymphoid cells under conditions of low toxin concentration. For these studies, we employed another lymphoid cell line, CCRF-CEM; we determined that the optimal dose of Cdt for G2 arrest at 16 h was 200 pg ml^{-1}. Under these conditions, we failed to detect H2AX phosphorylation at 4 h of exposure while treatment with a known DDR activator, etoposide, caused significant increases in pH2AX. Moreover, the use of ATM inhibitors (KU60019 and KU55933) failed to alter Cdt-induced G2 arrest, whereas cell cycle arrest and H2AX phosphorylation due to etoposide exposure were reduced by these inhibitors. Clearly, these results do not support the role for activation of the DDR in association with Cdt-mediated toxicity of lymphoid cells.

In order to determine if the lipid phosphatase activity associated with CdtB and the resultant PI-3K blockade also contributed to toxicity in non-lymphoid cells, HeLa cells, a well-established experimental target cell to study the actions of Cdt, were examined. Under conditions optimized to induce cell cycle arrest at 24 h (25 ng ml^{-1} of each of the Cdt subunits), we observed significant phosphorylation of H2AX at 16 h in the presence of CdtB^{WT}. In contrast, when the wild-type protein was substituted with CdtB^{A163R}, the mutant retaining significant phosphatase but lacking DNase activity, we failed to detect a significant increase in pH2AX. It should be noted that this mutant did induce G2 arrest at levels comparable with those of CdtB^{WT}. Thus, HeLa cells were able to undergo Cdt-induced G2 arrest in the absence of CdtB-associated DNase activity and detectable DDR activation. These results are consistent with those of Sert *et al*. (1999) who demonstrated that Cdt-induced G2 arrest in HeLa cells was independent of DNA damage. We also examined other CdtB mutants that retained DNase activity but exhibited significantly reduced phosphatase activity; these were not able to induce cell cycle arrest or increases in pH2AX in HeLa cells. In addition to reductions in PIP3 and pGSK3β, further evidence for the role of PI-3K blockade was demonstrated by the ability of the GSK Inhibitor XV to block toxin-induced G2 arrest in HeLa cells as observed for lymphoid cells. One feature of Cdt's effect on HeLa cells that differs from lymphoid cells is the extent of PIP3 depletion. In the case of lymphoid cells, PIP3 levels were reduced to 70–80% in the presence of 20–5000 pg ml^{-1} quantities of toxin; in contrast, HeLa cells required 5–50 ng ml^{-1} of toxin to achieve a smaller reduction (30%). It is interesting to note that the level of reduction observed for pGSK3β in HeLa cells mirrored the effects observed for PIP3. This difference in PIP3 depletion may contribute to the requirement for higher doses of Cdt required to intoxicate HeLa cells as reported by several investigators (Deng *et al*., 2001; Li *et al*., 2002; Guerra *et al*., 2011). One possible explanation, suggested by several investigators, is that PI-3K is constitutively active in HeLa cells (Kang *et al*., 2012; Jin *et al*., 2014). In contrast, lymphocytes typically exhibit low levels of PI-3K activity with transient increases upon activation; moreover, the sustained elevated levels of PIP3 in Jurkat cells result from deficiencies in its degradation attributed to decreased expression of both PIP3 phosphatases: PTEN and SHIP1 (Seminario *et al*., 2003; Shan *et al*., 2010).

Our results do not, however, rule out the possible influence of DNase activity under conditions of exposure to high concentrations of toxin for different periods of time as reported by other investigators (Deng *et al*., 2001; Li *et al*., 2002; Guerra *et al*., 2011). Moreover, it is becoming increasingly clear that all cell types susceptible to Cdt do not respond to the toxin in the same manner with some cells rapidly becoming apoptotic and others arresting in either the G1 or G2 phase of the cell cycle (Cortes-Bratti *et al*., 2001b). Thus, it is possible that the underlying cause of this variability, and the relative role of lipid phosphatase versus DNase activity of CdtB, could be determined by cell types and their relative dependence on PI-3K signalling. For instance, Rabin *et al*. (2009) reported that a CdtB mutant involving residue H160 (CdtB^{H160Q}) exhibited a decrease in PIP3 phosphatase activity and reduced toxicity for proliferating cells but retained the capacity to induce apoptosis in nonproliferating macrophages. It should be noted that these cells failed to exhibit caspase activation and apoptosis-inducing factor release. Thus, it is not clear if this represents a differential effect involving proliferating versus nonproliferating cells or the investigators' failure to detect phosphatase activity because they were measuring substrate consumption as opposed to the generation of enzymatic product. Indeed, our own studies indicate that nonproliferating cells are not susceptible to Cdt-induced apoptosis (Shenker *et al*., 2001; 2010a; 2014). In other studies, Frisan *et al*. (2003) suggest that PI-3K activation is required for the cellular distension observed in Cdt-treated HeLa cells. Unfortunately, these authors did not provide direct evidence for activation of the PI-3K cascade such as altered phosphorylation and activity of downstream targets. In this context, it is also important to note that Lee *et al*. (2006) demonstrated that while the regulation of cell size is dependent upon PI-3K signalling and mammalian target of rapamycin activation, there is a disconnect between cell size regulation and the ability of cells to undergo cell cycle arrest. These observations are particularly relevant to our study as cellular distension is not a prominent feature of Cdt-induced lymphocyte cell cycle arrest. Finally, it should be noted that *Saccharomyces cerevisiae* are susceptible to Cdt-induced cell cycle arrest (Hassane *et al*., 2001; Matangkasombut *et al*., 2010). These observations are of

interest as these cells do not produce PIP3; nonetheless, they do produce, and are dependent upon, a myriad of phosphatidylinositol monophosphate and diphosphates for several functions including growth and survival (Gardocki *et al*., 2005; Strahl and Thorner, 2007). It is possible that CdtB is capable of altering one or more of these moieties in *S. cerevisiae*, although it should be noted that we have not observed such effects in lymphoid cells or in a cell-free system.

Collectively, our observations support a critical role for the lipid phosphatase activity associated with CdtB in mediating G2 arrest. Several lines of evidence support the candidacy of PIP3 as the primary molecular target of CdtB, particularly in lymphoid cells and possibly in HeLa cells as well. First, as previously noted, CdtB's *in vitro* PIP3 phosphatase activity is much more robust than its nuclease activity (Shenker *et al*., 2007). Second, it appears that the ability of CdtB and its mutants to induce cell toxicity always correlates with retention of relatively high levels of phosphatase activity and not DNase activity. The $CdtB^{A163R}$ mutant, in particular, retains the ability to induce G2 arrest even though it fails to stimulate DNA damage. Finally, we have now demonstrated that cells exposed to Cdt exhibit downstream changes consistent with the action of a PIP3 phosphatase: decreases in PIP3, increases in PI-3,4P2 and decreased phosphorylation of Akt and GSK3β leading to a respective loss and gain of kinase activity. The observations of Carette *et al*. (2009) support, albeit indirectly, the role of CdtB in cell signalling and lipid metabolism as these results are much easier to explain in the context of PIP3 phosphatase activity of CdtB. Nonetheless, our studies do not eliminate the possibility that Cdt may indeed exhibit dual enzymatic functions. DNase activity of CdtB may contribute to toxicity in some cell types that do not employ PIP3 signalling, particularly when exposed to high doses of toxin, while lipid phosphatase activity is critical for toxicity in other cells such as lymphocytes that rely heavily on PIP3 signalling.

Experimental procedures

Cell culture, cell cycle and phospho-H2AX analysis

The human leukaemic T cell line, Jurkat (E6-1), was maintained in RPMI-1640 supplemented with 10% foetal calf serum, 2 mM of glutamine, 10 mM of HEPES, 100 U ml^{-1} of penicillin and 100 μg ml^{-1} of streptomycin. Cells were harvested in mid-log growth phase and plated at 5×10^5 cells per millilitre, or as indicated, in 24-well tissue culture plates. Cells were exposed to medium, Cdt peptides or Cdt holotoxin and incubated for times indicated.

Human peripheral blood mononuclear cells lymphocytes were prepared as described previously (Shenker *et al*., 1982a). Briefly, HPBMC were isolated from 100 to 200 ml of heparinized venous blood obtained from healthy donors. HPBMC were isolated by buoyant density centrifugation on Ficoll-Paque (Amersham Pharmacia Biotech; Piscataway, NJ). Lymphocytes (1×10^6 cells per millilitre) were activated with 1 μg ml^{-1} PHA (Abbott Laboratories, Chicago, IL) following pre-treatment for 45 min with Cdt; the cells were incubated in RPMI-1640, antibiotics and 2% heat-inactivated human AB sera for the periods of time indicated.

HeLa cells (CRL-1958; ATCC) were cultured in minimal essential medium supplemented with 10% foetal bovine serum and 2% antibiotic solution at 37°C in 5% CO_2. The cells were seeded at 2×10^5 cells per well in a 12-well plate and allowed to attach 1 day prior to experimental treatment. Following the exposure, cells were trypsinized and analysed as described in the following.

To measure Cdt-induced cell cycle arrest, cells were incubated for the times indicated and then washed and fixed for 60 min with cold 80% ethanol (Shenker *et al*., 2005). The cells were stained with 10 μg ml^{-1} of propidium iodide containing 1 mg ml^{-1} of RNase (Sigma-Aldrich, St. Louis, MO) for 30 min. Samples were analysed on a Becton-Dickinson LSRII flow cytometer (BD Biosciences, Franklin Lakes, NJ) as previously described (Shenker *et al*., 2005). A minimum of 15 000 events were collected for each sample; cell cycle analysis was performed using Modfit (Verity Software House, Topsham, ME).

To measure pH2AX, cells were incubated with the toxin for 4 h (Jurkat cells) or 16 h (HeLa cells), collected and fixed with 4% paraformaldehyde in phosphate-buffered saline (PBS) for 30 min at room temperature. Cells were washed, permeabilized (0.3% Triton X-100) and blocked [PBS containing 1% bovine serum albumin (BSA)] for 1 h at room temperature. Cells were stained with pH2AX (S139) rabbit monoclonal antibody conjugated to Alexa Fluor 488 (Cell Signaling Technology, Danvers, MA) in PBS containing 1% BSA and 0.3% Triton X-100 overnight at 4°C. Control samples were incubated with rabbit IgG isotype control (Cell Signaling Technology). After washing, cells were analysed by flow cytometry as described earlier.

Construction of plasmid containing CdtB mutant genes

Amino acid substitutions were introduced into the *cdtB* gene by *in vitro* site-directed mutagenesis using oligonucleotide primer pairs containing appropriate base changes (Table 1). Site-directed mutagenesis was performed using the QuikChange II site-directed mutagenesis kit (Stratagene, La Jolla, CA) according to the manufacturer's directions. Amplification of the mutant plasmid was carried out using PfuUltra HF DNA polymerase (Stratagene). All mutants involving a single amino acid utilized pGEMCdtB as a template; construction and characterization of this plasmid were previously described (Shenker *et al*., 2005). $pGEMCdtB^{R117A•R144A•N201A}$ was achieved by first constructing a double-mutant-containing plasmid, $pGEMCdtB^{R117A•R144A}$, using $pGEMCdtB^{R117A}$ as a template (Shenker *et al*., 2007) and primers P3 and P4 (Table 1) for $pGEMCdtB^{R144A}$; the double mutant was then used as a template to construct $pGEMCdtB^{R117A•R144A•N201A}$ with primers P7 and P8. The triple-mutant-containing plasmid $pGEMCdtB^{F156I•T158A•A163R}$

was constructed using pGEMCdtB^{A163H} as a template, along with primers P9 and P10. Finally, pGEMCdtB$^{Y239R•A240I•D244G•H246L}$ was achieved by first constructing pGEMCdtB$^{Y239R•A240I}$ with primers P3 and P4 using pGEMCdtB as a template; the resulting pGEMCdtB$^{Y239R•A240I}$ plasmid was then used as a template in conjunction with primers P15 and P16. All mutants were verified by DNA sequencing.

Expression and purification of Cdt peptides, CdtB mutants and Cdt holotoxin

In vitro expression of Cdt peptides and CdtB mutants was performed using the Rapid Translation System (RTS 500 ProteoMaster; Roche Diagnostics Corp, Indianapolis, IN) as previously described (Shenker *et al.*, 2005). Reactions were run according to the manufacturer's specification (Roche Diagnostics Corp) using 10–15 μg of template DNA. After 20 h at 30°C, the reaction mix was removed, and the expressed Cdt peptides were purified by nickel affinity chromatography as described (Shenker *et al.*, 2005).

Construction and expression of the plasmid containing the *cdt* genes for the holotoxin (pUCAacdtABC^{his}) have previously been reported (Shenker *et al.*, 2004). The plasmid was constructed so that *cdt* genes were under control of the *lac* promoter and transformed into *E. coli* DH5α. Cultures of transformed *E. coli* were grown in 1L LB broth and induced with 0.1 mM of isopropyl β-D-1-thiogalactopyranoside for 2 h; bacterial cells were harvested, washed and resuspended in 50 mM of Tris (pH 8.0). The cells were frozen overnight, thawed and sonicated. The histidine-tagged peptide holotoxin was isolated by nickel affinity chromatography as previously described (Shenker *et al.*, 2000).

Phosphatase assay

Phosphatase activity was assessed by monitoring the dephosphorylation of PIP3 as previously described (Maehama *et al.*, 2000; Shenker *et al.*, 2007). Briefly, the reaction mixture (20 μl) consisted of 100 mM of Tris-HCl (pH 8.0), 10 mM of dithiothreitol, 0.5 mM of diC16-phosphatidylserine (Avanti Polar Lipids, Alabaster, AL), 25 μM of PIP3 (Echelon Biosciences, Salt Lake City, UT) and the indicated amount of CdtB^{WT} or mutant. Appropriate amounts of lipid solutions were deposited in 1.5 ml tubes, organic solvent removed, the buffer added and a lipid suspension formed by sonication. Phosphatase assays were carried out at 37°C for 30 min; the reactions were terminated by the addition of 15 μl of 100 mM *N*-ethylmaleimide. Inorganic phosphate levels were then measured using a malachite green assay.

DNase assay

CdtB peptides were assessed for DNase activity by monitoring changes in electrophoretic mobility of supercoiled plasmid DNA as described by Elwell and Dreyfus (2000). Briefly, supercoiled pUC19 (1 μg per reaction) was incubated with CdtB, CdtB mutants or bovine DNase I for 4 h at 37°C in a buffer containing 25 mM of Hepes (pH 7.0), 10 mM of $MgCl_2$ and 5 mM of $CaCl_2$. The reaction was stopped by adding 10 mM of EDTA (final concentration). The samples were then loaded onto 1% agarose gel and subjected to electrophoresis in Tris–borate–EDTA buffer; gels were stained with ethidium bromide and analysed by digital scanning densitometry.

Measurement of cellular PIP3, PI-3,4-P2 and PI-3,5-P2 content

Cells (1×10^6 ml^{-1}) were incubated in the presence of medium or Cdt for 0–240 min. Replicate cultures ($0.5–1 \times 10^7$ cells) were pooled and harvested. The cell pellet was treated with cold 0.5 trichloroacetic acid (TCA) for 5 min and centrifuged and the pellet washed twice with 5% TCA containing 1 mM of EDTA. Neutral lipids were extracted twice with methanol : chloroform (2:1) at room temperature (RT). Acidic lipids were extracted with methanol : chloroform : 12M HCl (80:40:1) for 15 min at RT; the samples were centrifuged for 5 min and the supernatant recovered. The supernatant was then treated with 0.75 ml of chloroform and 0.1 M of HCl and centrifuged to separate organic and aqueous phases; the organic phase was collected and dried. The dried lipids were resuspended in 120 μl of 50 mM HEPES buffer (pH 7.4) containing 150 mM of NaCl and 1.5% sodium cholate and left overnight at 4°C. PI-3,4,5-P_3, PI-3,4-P2 and PI-4,5-P2 levels were then determined using commercially available competitive enzyme-linked immunosorbent assay according to the manufacturer's directions (Echelon Biosciences).

Docking experiments

Docking experiments were performed using AutoDock and analysed with AutoDockTools (Morris *et al.*, 2009). Both IP3 and IP2 were tested as ligands. After adding hydrogens to CdtB (pdb code 2f2f, chain B) and the ligand, we performed docking where most of the protein was held rigid. The ligand was allowed to be flexible, as well as 15 amino acids in a radius of 8 Å around His274 (the presumed active site of CdtB). We typically recorded 500–1000 docking conformations, and the ligands from lowest-energy complexes were clustered and visualized either with AutoDockTools or PyMol (PyMol Graphics System, Schrödinger, LLC, New York, NY). Representative docking simulations are shown in Figs. S1 and S2; these results helped us identify amino acids that are potentially involved in substrate binding. This information was used as a guide in our mutagenesis experiments.

Measurement of cellular content of Akt and GSK3β and kinase activity

Cells were treated as described and solubilized in 20 mM of Tris-HCl buffer (pH 7.5) containing 150 mM of NaCl, 1 mM of EDTA, 1% NP-40, 1% sodium deoxycholate and protease inhibitor cocktail (ThermoFisher Scientific, Grand Island, NY). Samples (30 μg) were separated on 12% sodium dodecyl sulfate polyacrylamide gel electrophoresis and then transferred to nitrocellulose. The membrane was blocked with BLOTTO and then incubated with one of the following primary antibodies for 18 h at 4°C (Shenker *et al.*, 1999): anti-pAkt (S473), anti-pGSK3β (S9) (Cell Signaling Technology) or anti-actin (Santa Cruz Biotechnology, Dallas, TX). Membranes were incubated with goat anti-mouse immunoglobulin

conjugated to horseradish peroxidase (SouthernBiotech, Birmingham, AL). The Western blots were developed using chemiluminescence and analysed by digital densitometry (Kodak Image Systems Rochester, NY) as previously described (Shenker *et al*., 2010b).

Jurkat cells (2×10^6) were incubated for 2 h in the presence of medium or Cdt as indicated. Cells were washed and fixed in 2% formaldehyde and permeabilized using commercially available fixative and permeabilization buffer (BD Biosciences). Cells were then stained with anti-Akt conjugated to AF647 (BD Biosciences) or with anti-pGSK3β (Ser9); the latter was detected with goat anti-rabbit antisera conjugated to fluorescein isothiocyanate (BD Biosciences). Cells were then analysed by flow cytometry; 10 000 events were collected (Boesze-Battaglia *et al*., 2006).

Akt-specific and GSK3β-specific kinase activity was assessed in control and Cdt-treated cells. Jurkat cells (2×10^6) were treated with Cdt as described; replicate cultures pooled and solubilized. Akt activity was measured using a commercially available assay kit (Cell Signaling Technology). Briefly, Akt was immunoprecipitated, and the enzyme was assessed for its ability to phosphorylate GSK3β *in vitro*; activity was monitored by Western blot. GSK3β kinase activity was also measured using a commercially available kit (Sigma-Aldrich). The kinase was immunoprecipitated and activity determined by following the utilization of ^{32}P-ATP to phosphorylate a synthetic substrate.

Statistical analysis

Mean ± standard error of the mean were calculated for replicate experiments. Significance was determined using Student's *t*-test; a *P*-value of less than 0.05 was considered to be statistically significant.

Acknowledgments

We thank the SDM Flow Cytometry Facility for its support of these studies. This work was supported by the National Institutes of Health (DE06014 and DE-023071).

References

Boesze-Battaglia, K., Besack, D., McKay, T.L., Zekavat, A., Otis, L., Jordan-Sciutto, K., *et al*. (2006) Cholesterol-rich membrane microdomains mediate cell cycle arrest induced by *Actinobacillus actinomycetemcomitans* cytolethal distending toxin. *Cell Microbiol* **8**: 823–836.

Boesze-Battaglia, K., Brown, A., Walker, L., Besack, D., Zekavat, A., Wrenn, S., *et al*. (2009) Cytolethal distending toxin-induced cell cycle arrest of lymphocytes is dependent upon recognition and binding to cholesterol. *J Biol Chem* **284**: 10650–10658.

Buckler, J., Liu, X., and Turka, L.A. (2008) Regulation of T-cell responses by PTEN. *Immunol Rev* **224**: 239–248.

Cantley, L., and Neel, B. (1999) New insights into tumor suppression: PTEN suppresses tumor formation by restraining the phosphoinositide 3 kinase/Akt pathway. *Proc Natl Acad Sci* **96**: 4240–4245.

Carette, J., Guimaraes, C., Varadarajan, M., Park, A., Wuethrich, I., Godarova, A., *et al*. (2009) Haploid genetic screens in human cells identify host factors used by pathogens. *Science* **236**: 1231–1234.

Coers, W., Vos, J.T.W.M., Van der Meide, P.H., Van der Horst, M.L.C., Huitema, S., and Weening, J.J. (1995) Interferon-gamma (IFN-y) and IL-4 expressed during mercury-induced membranous mephropathy are toxic for cultured podocytes. *Clin Exp Immunol* **102**: 297–307.

Comayras, C., Tasca, C., Peres, S.Y., Ducommun, B., Oswald, E., and De Rycke, J. (1997) *Escherichia coli* cytolethal distending toxin blocks the HeLa cell cycle at the G2/M transition by preventing cdc2 protein kinase dephosphorylation and activation. *Infect Immun* **65**: 5088–5095.

Cortes-Bratti, X., Frisan, T., and Thelestam, M. (2001a) The cytolethal distending toxins induce DNA damage and cell cycle arrest. *Toxicon* **39**: 1729–1736.

Cortes-Bratti, X., Karlsson, C., Lagergard, T., Thelastam, M., and Frisan, T. (2001b) The *Haemophilus ducreyi* cytolethal distending toxin induces cell cycle arrest and apoptosis via the DNA damage checkpoint pathways. *J Biol Chem* **276**: 5296–5302.

Deng, K., Latimer, J., Lewis, D., and Hansen, J.C. (2001) Investigation of the interaction among the components of the cytolethal distending toxin of *Haemophilus ducreyi*. *Biochem Biophys Res Commun* **285**: 609–615.

Dlakic, M. (2000) Functionally unrelated signalling proteins contain a fold similar to Mg^{2+}-dependent endonucleases. *Trends Biochem Sci* **25**: 272–273.

Dlakic, M. (2001) Is CdtB a nuclease or a phosphatase? *Science* **291**: 547.

Drayer, A., Pesesse, X., De Smedt, F., Communi, D., Moreau, G., and Erneux, C. (1996) The family of inositol and phosphatidylinositol polyphosphate 5-phosphatases. *Biochem Soc Trans* **24**: 1001–1005.

Elwell, C.A., Chao, K., Patel, K., and Dreyfus, L.A. (2001) *Escherichia coli* CdtB mediates cytolethal distending toxin cell cycle Arrest. *Infect Immun* **69**: 3418–3422.

Elwell, C.A., and Dreyfus, L.A. (2000) DNase I homologous residues in CdtB are critical for cytolethal distending toxin-mediated cell cycle arrest. *Mol Microbiol* **37**: 952–963.

Frisan, T., Cortes-Bratti, X., and Thelestam, M. (2002) Cytolethal distending toxins and activation of DNA damage-dependent checkpoint responses. *Int J Med Microbiol* **291**: 495–499.

Frisan, T., Cortes-Bratti, X., Chaves-Olarte, E., Stenerlow, B., and Thelastam, M. (2003) The *Haemophilus ducreyi* cytolethal distending toxin induces DNA double-strand breaks and promotes ATM-dependent activation of RhoA. *Cell Microbiol* **5**: 695–707.

Frisk, A., Lebens, M., Johansson, C., Ahmed, H., Svensson, L., Ahlman, K., *et al*. (2001) The role of different protein components from the *Haemophilus ducreyi* cytolethal distending toxin in the generation of cell toxicity. *Microb Pathog* **30**: 313–324.

Gardocki, M., Jani, N., and Lopes, J. (2005) Phosphatidylinositol biosynthesis: biochemistry and regulation. *Biochim Biophys Acta* **1735**: 89–100.

Gelfanova, V., Hansen, E., and Spinola, S. (1999) Cytolethal distending toxin of *Haemophilus ducreyi* induces apoptotic death of Jurkat T cells. *Infect Immun* **67**: 6394–6402.

Guerra, L., Buidi, R., Slot, I., Callegari, S., Sompallae, R., Pickett, C., *et al*. (2011) Bacterial genotoxin triggers FEN1-

dependent RhpA activation, cytoskeleton remodeling and cell survival. *J Cell Sci* **124**: 2732–2742.
Guerra, L., Carr, H., Richter-Dahlfors, A., Masucci, M., Thelestam, M., Forst, J., *et al*. (2008) A bacterial cytotoxin identifies the RhoA exchange factor Net1 as a key effector in the response to DNA damage. *PLoS One* **3**: e2254.
Hassane, D., Lee, R., and Pickett, C.L. (2005) *Campylobacter jejuni* cytolethal distending toxin promotes DNA repair responses in normal human cells. *Infect Immun* **71**: 541–545.
Hassane, D., Lee, R., Mendenhall, M., and Pickett, C. (2001) Cytolethal distending toxin demonstrates genotoxic activity in a yeast model. *Infect Immun* **69**: 5752–5759.
Huang, Y., and Sauer, K. (2010) Lipid signaling in T cell development and function. *Cold Spring Harb Perspect Biol* **2**: 1–25.
Jin, Y., Xu, T., Zhao, Y., Wang, Y., and Cui, M. (2014) In vitro and in vivo anti-cancer activity of formononetin on human cervical cancer cell line HeLa. *Tumor Biol* **35**: 2279–2284.
Kang, S., Dong, S., Kim, B., Park, M., Trink, B., Byun, H., *et al*. (2012) Thioridazine induces apoptosis by targeting the PI3K/Akt/mTor pathway in cervical and endometrial cancer cells. *Apoptosis* **17**: 989–997.
Kraub, M., and Haucke, V. (2007) Phosphoinositides: regulators of membrane traffic and protein function. *FEBS Lett* **581**: 2105–2111.
Krystal, G. (2000) Lipid phosphatases in the immune system. *Semin Immunol* **12**: 397–403.
Lahm, A., and Suck, D. (1991) DNase I-induced DNA conformation. 2 Å structure of a DNase I-octamer complex. *J Mol Biol* **222**: 645–667.
Lara-Tejero, M., and Galan, J.E. (2000) A bacterial toxin that controls cell cycle progression as a deoxyribonuclease I-like protein. *Science* **290**: 354–357.
Lee, C.-H., Inoki, K., and Guan, K.-L. (2006) mTOR pathway as a target in tissue hypertrophy. *Annu Rev Pharmacol Toxicol* **47**: 443–467.
Li, L., Sharip, A., Chaves-Olarte, E., Masucci, M., Levitsky, V., Thelestam, M., *et al*. (2002) The *Haemophilus ducreyi* cytolethal distending toxin activates sensors of DNA damage and repair complexes in proliferating and non proliferating cells. *Cell Microbiol* **4**: 87–99.
Liscovitch, M., and Cantley, L. (1992) Lipid second messengers. *Cell* **77**: 329–334.
Luo, J. (2009) Glycogen synthase kinase 3β (GSK3β) in tumorigenesis and cancer chemotherapy. *Cancer Lett* **273**: 194–200.
Maehama, T., Taylor, G., Slama, J., and Dixon, J. (2000) A sensitive assay for phosphoinositide phosphatases. *Anal Biochem* **279**: 248–250.
Majerus, P., Kisseleva, M., and Norris, F. (1999) The role of phosphatases in inositol signaling reactions. *J Biol Chem* **274**: 10669–10672.
Mao, X., and DiRienzo, J.M. (2002) Functional studies of the recombinant subunits of a cytolethal distending toxin. *Cell Microbiol* **4**: 245–255.
March, M., and Ravichandran, K. (2002) Regulation of the immune response by SHIP. *Semin Immunol* **14**: 37–47.
Matangkasombut, O., Wattanawaraporn, R., Tsuruda, K., Ohara, M., Sugai, M., and Mongkolsuk, S. (2010) Cytolethal distending toxin from *Aggregatibacter actinomycetemcomitans* induces DNA damage, S/G_2 cell cycle arrest, and caspase-independent death in a *Saccharomyces cerevisiae* model. *Infect Immun* **78**: 783–792.
Mayer, M., Bueno, L., Hansen, E., and DiRienzo, J.M. (1999) Identification of a cytolethal distending toxin gene locus and features of a virulence-associated region in *Actinobacillus actinomycetemcomitans*. *Infect Immun* **67**: 1227–1237.
Mitchell, C., Brown, S., Campbell, J., Munday, A., and Speed, C. (1996) Regulation of second messengers by the inositol polyphosphate 5-phosphatases. *Biochem Soc Trans* **24**: 994–1000.
Morris, G., Huey, R., Lindstrom, W., Sanner, M., Belew, R., Goodsell, D., *et al*. (2009) AutoDock4 and AutoDockTools4: Automated docking with selective receptor flexibility. *J Comput Chem* **16**: 2785–2791.
Nalbant, A., Chen, C., Wang, Y., and Zadeh, H.H. (2003) Induction of T-cell apoptosis by *Actinobacillus actinomycetemcomitans* mutants with deletion of *ltxA* and cdtABC genes: possible activity of. *Oral Microbiol Immunol* **18**: 339–349.
Nesic, D., Hsu, Y., and Stebbins, C.E. (2004) Assembly and function of a bacterial genotoxin. *Nature* **429**: 429–433.
Ohara, M., Hayashi, T., Kusonoki, Y., Miyauchi, M., Takata, T., and Sugai, M. (2004) Caspase-2 and caspase-7 are involved in cytolethal distending toxin-induced apoptosis in Jurkat and MOLT-4 T-cell lines. *Infect Immun* **72**: 871–879.
Okuda, J., Kurazono, H., and Takeda, Y. (1995) Distribution of the cytolethal distending toxin A gene (cdtA) among species of *Shigella* and *Vibrio*, and cloning and sequencing of the cdt gene from *Shigella dysenteriae*. *Microb Pathog* **18**: 167–172.
Pickett, C.L., Pesci, E.C., Cottle, D.L., Russell, G., Erdem, A. N., and Zeytin, H. (1996) Prevalence of cytolethal distending toxin production in *Campylobacter jejuni* and relatedness of *Campylobacter* sp. cdtB gene. *Infect Immun* **64**: 2070–2078.
Rabin, S., Flitton, J., and Demuth, D.R. (2009) *Aggregatibacter actinomycetemcomitans* cytolethal distending toxin induces apoptosis in nonproliferating macrophages by a phosphatase-independent mechanism. *Infect Immun* **77**: 3161–3169.
Rayasam, G., Tulasi, V., Sokhi, R., Davis, J., and Ray, A. (2009) Glycogen synthase kinase 3: more than a namesake. *Br J Pharmacol* **156**: 885–898.
Sasaki, T., Sasaki, J., Sakai, T., Takasuga, S., and Suzuki, A. (2007) The physiology of phosphoinositides. *Biol Pharm Bull* **30**: 1599–1604.
Scott, D.A., and Kaper, J.B. (1994) Cloning and sequencing of the genes encoding *Escherichia coli* cytolethal distending toxin. *Infect Immun* **62**: 244–251.
Seminario, M., and Wange, R. (2003) Lipid phosphatases in the regulation of T cell activation: living up to their PTEN-tial. *Immunol Cell Biol* **192**: 80–97.
Seminario, M.C., Precht, P., Wersto, R., Gorospe, M., and Wange, R.L.. (2003) PTEN expression in PTEN-null leukaemic T cell lines leads to reduced proliferation via slowed cell cycle progression. *Oncogene* **22**: 8195–8204.
Sert, V., Cans, C., Tasca, C., Bret-Bennis, L., Oswald, E., Ducommun, B., *et al*. (1999) The bacterial cytolethal distending toxin (CDT) triggers a G2 cell cycle checkpoint in mammalian cells without preliminary induction of DNA strand breaks. *Oncogene* **18**: 6296–6304.

Shan, X., Czar, M., Bunnel, S., Liu, P., Liu, Y., Schwartzberg, P., *et al*. (2010) Deficiency of PTEN in Jurkat T cells causes constitutive localization of Itk to the plasma membrane and hyperresponsiveness to CD3 stimulation. *Mol Cell Biol* **20**: 6945–6957.

Shenker, B.J., Ali, H., and Boesze-Battaglia, K. (2011) PIP3 regulation as promising targeted therapy of mast cell mediated diseases. *Curr Pharm Des* **17**: 3815–3822.

Shenker, B.J., Besack, D., McKay, T.L., Pankoski, L., Zekavat, A., and Demuth, D.R. (2004) *Actinobacillus actinomycetemcomitans* cytolethal distending toxin (Cdt): evidence that the holotoxin is composed of three subunits: CdtA, CdtB, and CdtC. *J Immunol* **172**: 410–417.

Shenker, B.J., Besack, D., McKay, T.L., Pankoski, L., Zekavat, A., and Demuth, D.R. (2005) Induction of cell cycle arrest in lymphocytes by *Actinobacillus actinomycetemcomitans* cytolethal distending toxin requires three subunits for maximum activity. *J Immunol* **174**: 2228–2234.

Shenker, B.J., Demuth, D.R., and Zekavat, A. (2006) Exposure of lymphocytes to high doses of *Actinobacillus actinomycetemcomitans* cytolethal distending toxin induces rapid onset of apoptosis-mediated DNA fragmentation. *Infect Immun* **74**: 2080–2092.

Shenker, B.J., Dlakic, M., Walker, L., Besack, D., Jaffe, E., Labelle, E., *et al*. (2007) A novel mode of action for a microbial-derived immunotoxin: the cytolethal distending toxin subunit B exhibits phosphatidylinositol (3,4,5) tri-phosphate phosphatase activity. *J Immunol* **178**: 5099–5108.

Shenker, B.J., Hoffmaster, R.H., McKay, T.L., and Demuth, D.R. (2000) Expression of the cytolethal distending toxin (Cdt) operon in *Actinobacillus actinomycetemcomitans*: evidence that the CdtB protein is responsible for G2 arrest of the cell cycle in human T-cells. *J Immunol* **165**: 2612–2618.

Shenker, B.J., Hoffmaster, R.H., Zekavat, A., Yamguchi, N., Lally, E.T., and Demuth, D.R. (2001) Induction of apoptosis in human T cells by *Actinobacillus actinomycetemcomitans* cytolethal distending toxin is a consequence of G_2 arrest of the cell cycle. *J Immunol* **167**: 435–441.

Shenker, B.J., McArthur, W.P., and Tsai, C.C. (1982a) Immune suppression induced by *Actinobacillus actinomycetemcomitans*. I. Effects on human peripheral blood lymphocyte responses to mitogens and antigens. *J Immunol* **128**: 148–154.

Shenker, B.J., McKay, T.L., Datar, S., Miller, M., Chowhan, R., and Demuth, D.R. (1999) *Actinobacillus actinomycetemcomitans* immunosuppressive protein is a member of the family of cytolethal distending toxins capable of causing a G2 arrest in human T cells. *J Immunol* **162**: 4773–4780.

Shenker, B.J., Tsai, C.-C., and Taichman, N.S. (1982b) Suppression of lymphocyte responses by *Actinobacillus actinomycetemcomitans*. *J Periodontal Res* **17**: 462–465.

Shenker, B.J., Vitale, L., and King, C. (1995) Induction of human T cells that co-express CD4 and CD8 by an immunomodulatory protein produced by *Actinobacillus actinomycetemcomitans*. *Cell Immunol* **164**: 36–46.

Shenker, B.J., Vitale, L.A., and Welham, D.A. (1990) Immune suppression induced by *Actinobacillus actinomycetemcomitans*: Effects on immunoglobulin production by human B cells. *Infect Immun* **58**: 3856–3862.

Shenker, B., Boesze-Battaglia, K., Zekavat, A., Walker, L., Besack, D., and Ali, H. (2010a) Inhibition of mast cell degranulation by a chimeric toxin containing a novel phosphatidylinositol-3,4,5-triphosphate phosphatase. *Mol Immunol* **48**: 203–210.

Shenker, B., Boesze-Battaglia, K., Zekavat, A., Walker, L., Besack, D., and Ali, H. (2010b) Inhibition of mast cell degranulation by a chimeric toxin containing a novel phosphatidylinositol-3,4,5-triphosphate phosphatase. *Mol Immunol* **48**: 203–210.

Shenker, B., Walker, L., Zekavat, A., Dlakic, M., and Boesze-Battaglia, K. (2014) Blockade of the PI-3K signaling pathway by the *Aggregatibacter actinomycetemcomitans* cytolethal distending toxin induces macrophages to synthesize and secrete pro-inflammatory cytokines. *Cell Microbiol* **16**: 1391–1404.

Strahl, T., and Thorner, J. (2007) Synthesis and function of membrane phosphoinositides in budding yeast, *Saccharomyces cerevisiae*. *Biochim Biophys Acta* **1771**: 353–404.

Thelastam, M., and Frisan, T. (2004) Cytolethal distending toxins. *Rev Physiol Biochem Pharmacol* **152**: 111–133.

Tsujishita, Y., Guo, S., Stolz, L., York, J., and Hurley, H. (2001) Specificity determinants in phosphoinositide dephosphorylation: crystal structure of an archetypal inositol polyphosphate 5-phosphatase. *Cell* **105**: 379–389.

Woscholski, R., and Parker, P. (1997) Inositol lipid 5-phosphatases-traffic signals and signal traffic. *Trends Biochem Sci* **22**: 427–431.

Yamada, T., Komoto, J., Saiki, K., Konishi, K., and Takusagawa, F. (2006) Variation of loop sequence alters stability of cytolethal distending toxin (CDT): crystal structure of CDT from *Actinobacillus actinomycetemcomitans*. *Protein Sci* **15**: 362–372.

Yuan, T., and Cantley, L. (2008) PI3K pathway alterations in cancer: variations on a theme. *Oncogene* **27**: 5497–5510.

Supporting information

Additional Supporting Information may be found in the online version of this article at the publisher's web-site:

Fig. S1. Lowest-energy clusters of IP2 (17 conformations) and IP3 (21 conformations) are shown in panels A and C respectively. A single lowest-energy docked conformation of IP2 and IP3 is shown up close in panels B and D respectively. Ligand-interacting amino acid residues mutated in our study (R117, R144 and A163) are shown as light-blue sticks. Hydrogen bonds between amino acids and the ligand are represented by magenta dashed lines.

Fig. S2. Docking simulations were performed as described in Methods. The movie shows 500 different conformations of IP3 docked in the active site of CdtB.

Fig. S3. Effect of CdtB on pGSK3β levels in HPBMC. HPBMC were activated with PHA in the presence of medium or Cdt holotoxin (0–1000 pg ml–1) for 4 h; cells were then harvested, fractionated by SDS-PAGE and analysed by Western blot for pGSK3β, GSK3β and actin. Densitometry results are expressed as a percentage of control cells (medium only) and are represented by the numbers below each blot.

Fig. S4. Blockade of Cdt-induced G2 arrest in HPBMC by GSK3β inhibitor. HPBMC were incubated with medium alone (panel A), PHA alone (panel B), PHA plus 200 pg ml−1 of Cdt holotoxin (panel C) or PHA, Cdt holotoxin and GSK inhibitor X (50 μM) for 72 h. Cells were then stained with propidium iodide (PI) and analysed for cell cycle distribution; numbers represent the percentage of G2 cells. This is a representative experiment of three experiments each performed in triplicate.

Fig. S5. Effect of $CdtB^{WT}$ and $CdtB^{A163R}$ on pGSK3β in HeLa cells. HeLa cells were treated with 25 ng ml−1 of $CdtB^{WT}$ or $CdtB^{A163R}$ in the presence of 25 ng ml−1 of CdtA and CdtC for 4 h. The cells were then harvested, solubilized, fractionated by SDS-PAGE and analysed by Western blot for both pGSK3β (solid bars) and GSK3β (cross-hatched bars). Results are expressed as mean ± SEM relative intensity (% control) for three experiments; the asterisk indicates statistical significance ($p < 0.05$).